Efficiency Measurement of N95 Filtering Facepiece Respirators against Ultrafine Particles under Cyclic and Constant Flows

Alireza Mahdavi

A thesis

in

The Department of

Building, Civil and Environmental Engineering

Presented in Partial Fulfillment of the Requirements

for the Degree of Master of Applied Science (Civil Engineering) at

Concordia University

Montreal, Quebec, Canada

September 2013

CONCORDIA UNIVERSITY
School of Graduate Studies

This is to certify that the thesis prepared

By: ALIREZA MAHDAVI

Entitled: Efficiency Measurement of N95 Filtering Facepiece Respirators against Ultrafine Particles under Cyclic and Constant Flows

and submitted in partial fulfillment of the requirements for the degree of

Master of Applied Science (M.A.Sc)

complies with the regulations of the University and meets the accepted standards with respect to originality and quality.

Signed by the final examining committee:

DR. MARIA ELEKTOROWICZ Chair

DR. ZHI CHEN Examiner

DR. ALI DOLATABADI Examiner

DR. FARIBORZ HAGHIGHAT Supervisor

Approved by DR. MOHAMMED ZAHEERUDDIN
Chair of Department or Graduate Program Director

DR. CHRISTOPHER TRUEMAN
Dean of Faculty

Date 04 – Sep. – 2013

ABSTRACT

Efficiency Measurement of N95 Filtering Facepiece Respirators against Ultrafine Particles under Cyclic and Constant Flows

Alireza Mahdavi

Detrimental impacts associated with inhalation of ultrafine particles (UFPs) (diameter of particle, D_p <100 nm), on various respiratory organs, can be controlled by means of N95 filtering facepiece respirators (FFRs), widely used by industrial and healthcare workers. In this regard, investigation of N95 FFRs efficiency, against UFPs, under cyclic flow, in addition with constant flow, is very necessary, since cyclic flow represents actual breathing pattern.

The first objective of the thesis was to report the development of a procedure to investigate the individual impact of breathing frequency and flow rate on the performance of N95 FFRs. Experiments were performed for two peak inhalation flows (PIFs) (135 and 360 L/min) and two breathing frequencies (24 and 42 breaths per minute (BPM)) for a total of four cyclic flows. The results showed that, for the most penetrating particle size (MPPS) range, an increase in both PIF and breathing frequency could potentially enhance the penetration; however the effect of PIF was observed to be much more pronounced than frequency. Therefore, from low to high respiratory efforts, a huge portion of penetration enhancement was due to the PIF variations and only a small portion was contributed by the frequency variations.

With the second objective of the thesis, the penetrations measured with the cyclic flows (with mean inhalation flows (MIFs) ranging from 42 to 360 L/min) were compared with

those measured with the constant flows equal to the cyclic flow minute volume, mean inhalation flow (MIF) and peak inhalation flow (PIF). The results indicated that, for the MPPS, constant flows equal to the cyclic flow minute volume and PIF significantly underestimated and overestimated the penetration of cyclic flows, respectively. Constant flows equal to the MIFs of cyclic flows, however, resulted in closer penetrations compared to the cyclic flows. At higher flow rates, of course, the maximum penetrations under constant flow exceeded the maximum penetrations under cyclic flow (MIF).

With the third objective of the thesis, the impact of particle loading on the penetration was tested. Investigations were performed with a cyclic flow (with equivalent MIF of 170 L/min) and two constant flow rates (85 L/min and 170 L/min) for a period of 6-hour loading time. The results indicated that, for small particles (usually less than 100 nm), the particle loading effect lead to decrease in the penetration with the loading time. The MPPS was also found to shift towards larger sizes, as the respirators were loaded with more particles. For the final stage of loading, unlike the initial stage, the penetration of a large range of particles under cyclic flow was significantly higher than the penetrations under constant flow (equal to cyclic flow MIF).

AKNOWLEDGMENT

I would like to express my best thanks to my supervisor, Dr. Fariborz Haghighat, and my co-supervisor, Dr. Ali Bahloul of the Institut de recherche Robert-Sauvé en santé et en sécurité du travail (IRSST) for their great assistance and guidance towards my studies and completion of this dissertation. I would also like to have my best thanks to Dr. Claude Ostiguy, the IRSST, for his valuable guidance. Without their assistance and patience, this dissertation would never have been completed. Also, I wish to express many thanks to my thesis committee examiners: Dr. Ali Dolatabadi, Dr. Zhi Chen and Dr. Maria Elektorowicz for all their valuable and constructive suggestions towards the dissertation completion.

I wish to specially thank the scientific professional and physics engineer at the IRSST: Mr. Yves Cloutier; and the technicians: Mr. Pierre Drouin, Mr. Simon Demers and Mr. Gilles Paradis for all their valuable assistance to maintain various parts of the experimental setup; also express many thanks to Mrs. Diane Cormier for providing me with the materials required for the experiments. My sincere appreciations go to Dr. France Labréche and Ms. Mojgan Rajabi for helping me learn the fundamentals of statistical analysis I used along with my studies.

At last and the best, my sincerest appreciations, thanks and admirations go to my dearest people in my life: My parents for all their kindness and encouraging and strengthening supports; and my dear sister and brother, Saba and Amir Hosein.

TABLE OF CONTENTS

LIST OF FIGURES

LIST OF TABLES

LIST OF ABBREVIATIONS

Abbreviation	Description
ANOVA	Analysis of Variance
BPM	Breath per Minute
CFR	Code of Federal Regulations
CMD	Count Median Diameter
CPC	Condensation Particle Counter
DFM	Dust-Fume-Mist
DG SANCO	La Direction générale de la santé et des consommateurs
DMA	Differential Mobility Analyzer
DM	Dust-Mist
DOP	Dioctyl Phthalate
EC	Electrostatic Classifier
FFR	Filtering Facepiece Respirator
GSD	Geometric Standard Deviation
HEPA	High-Efficiency Particulate Air
IPA	Iso-propyl-alcohol (Iso-propanol)
ISO/TS	International Standard Organization, Technical Specification
MIF	Mean Inhalation Flow
Kr	Krypton
MMD	Mass Median Diameter
MPPS	Most Penetrating Particle Size
NaCl	Sodium Chloride

NAI	Negative Air Ion
NIOSH	National Institute for Occupational Safety and Health
NP	Nano-particles
NT	Nano-technology
PIF	Peak Inhalation Flow
PSL	Polystyrene Latex
RH	Relative Humidity
SMPS	Scanning Mobility Particle Sizer
UFPs	Ultrafine Particles

LIST OF SYMBOLS

Symbol	Description
C	Concentration
D_p	Particle Size
P	Penetration
Fr	Breathing Frequency
X_{PIF}	Enhancement Fraction Value (PIF)
X_{Fr}	Enhancement Fraction Value (Fr)

CHAPTER 1: INTRODUCTION

1.1 Overview

Ultrafine particles (UFPs) are referred to the particles which possess sizes less than 100 nm. There are two major sources for generation of UFPs: natural and man-made. Sea sprays and natural fumes resulting from the forest fires or volcano activities are common examples for the natural sources of UFPs (Oberdorster et al., 2005, Aitken et al., 2004). There are also man-made UFPs generated by secondary unvalued products. Welding fumes, for instance, generates vapors which condense considerable portions of liquefied metals in nano-structures (Hull and Abraham, 2002). Diesel fumes and aircraft exhaust are other types of man-made UFPs (Vincent and Clement, 2000, Teague, 2004).

Compared to UFPs (which are usually undesired produced materials), there are other sources of particles in nano-metric ranges (<100 nm) which are voluntarily produced. For instance, as a recently emerging phenomenon, nano-technology (NT) has lead to an industrial revolution, by production and manufacturing of a new generation of materials with high quality and specific characteristics. The estimation of the global market of products containing nano-materials, for example, will exceed 3 trillion $ by 2015 (Lux research, 2009, Maynard et al., 2011). Such a remarkable growth is consequently accompanied by creation and dispersion of a wide range of materials called nano-particles (NPs). A NP, by definition, is described as "*a nano-object with all three external dimensions in the size range from 1 to 100 nm*" (ISO/TS, 2009, Rengasamy et al., 2012). A NP can be synthesized by either formation of atom-atom or molecule-molecule groups constructed together (bottom-up approach) or by reducing the bulk of

materials by mechanical processes to reach the nano-scale structures (top-down approach) (Ostiguy et al., 2010). Air cleaning sprays, laser ablation, polishing, milling, surface coatings (spraying and deposition on the surface) and grinding are known as common sources of NPs (Rengasamy et al., 2008).

In addition with NPs and UFPs, several groups of bio-aerosols (airborne particles containing biological organisms) such as bacteria, viruses, virions and fungi are examples of natural products possessing the dimensions less than 100 nm (Ostiguy et al., 2010, Morawska, 2006, McCullough et al., 1997).

1.2 Concerns and Impacts

The exposure risk to UFPs and NPs and the potential health impacts is of more concern. The previous epidemiological studies have indicated the exposure to the particles with sizes less than 100 nm can result in severe respiratory and cardiovascular health effects (Penttinen et al., 2001, Wichmann et al., 2000). Nonetheless the information available regarding the epidemiological studies are more attributed to UFPs, rather than NPs, since, unlike UFPs, NPs have been recently emerged. Therefore the epidemiological studies regarding the health effect of NPs are still limited and further investigations, are highly needed (Ostiguy et al., 2008).

The main concern associated with exposure to the particles in nano-metric ranges, is their potential toxicity and their potential health impacts as, once inhaled, they can be deposited deeply into the alveolar section of the lungs, translocated to secondary target organs to generate inflammation and initiate the development of different diseases (Ostiguy et al., 2010, Maynard and Kuempel, 2005, Byrne and Baugh, 2008, Oberdorster

et al., 2004, 2002, Semmler et al., 2004). Many metrics must be used to estimate the toxicity of particles. The most important ones include: mass concentration, number concentration and surface area (Maynard and Aitken, 2007, Nel et al. 2006). Some toxicity studies of the UFPs and NPs found a good correlation between the surface area and the biological effects (Oberderoster et al., 2005, Faux et al., 2003, , Tran et al., 2000), while others found a better correlation between the number of particles and the biological effects (Churg et al., 2000). Less correlation, though, has been detected between mass concentration and biological effects. In addition, Oberdorster et al. (2000) and Donaldson et al. (2001) indicated that, for two samples of the 250 nm and 20 nm having the same mass concentration (10 $\mu g/cm^3$), the number concentrations are 1,200 $\#/cm^3$ and 2,400,000 $\#/cm^3$, respectively. Therefore a typical sample of UFPs or NPs is expected to have more adverse health effects compared with other sub-micrometer particle samples with the same mass.

1.3 Solutions to Control UFPs and NPs Exposure

Workers are naturally exposed to the UFPs and NPs by several ways such as production, manufacturing, use and disposal of nano-products (Aitkin et al., 2004, DG SANCO 2004). In such cases, the possible exposure routes are normally inhalation, eye contact, skin adsorption and dermal penetrations (Oberdorster et al., 2005). Among these routes, inhalation is considered as the most significant one (Mostofi et al., 2010). Available strategies such as exposure reduction time and local ventilation systems utilization are normally applied to control UFPs and NP exposure, however not always these strategies are able to provide the workers with an acceptable level of exposure. As the final strategy, the inhalation of harmful UFPs and NPs can be controlled by means filtering

facepiece respirators (FFRs) broadly employed by industrial and health-care workers. These filters are generally inexpensive, available and comfortable (Chen and Huang, 1998, Rengasamy et al., 2008).

In 1998, National Institute for Occupational Safety and Health (NIOSH) presented three classes of filter materials, each with three different levels of protection. These classes were N, R and P which were respectively referred as “non-resistant”, “resistant” and “proof” in terms of resistance against degradation by oil particulate matters (Rengasamy et al., 2011a). The protection levels were also 95, 99 and 100 which indicated the particle removal efficiency of 95, 99 and 99.97 %, respectively. Based on the protection efficiency level (95, 99 or 99.97 %) each class of N, R or P could be prefixed by 95, 99 or 100. NIOSH-certified filters (N, R and P classes) are classified to support the regulations of the 42 Code of Federal Regulations, Part 84 (42 CFR 84) which was replaced to modify 30 Code of Federal Regulations, Part 11 (30 CFR 11) in 1995. Following the 42 CFR 84 (subpart 181) and NIOSH regulations, N-class filters should be exposed to NaCl challenge concentration with count median diameter (CMD) of 75 nm and the maximum geometric standard deviation (GSD) of 1.86. P- and R-class filters should also be exposed to Dioctyle phthalate (DOP) particles with CMD of 165 nm and the maximum GSD of 1.6. Particles should be electrically neutralized to reflect the worst-case scenario. Based on the certifications by NIOSH and 42 CFR 84, filters are exposed to the constant air flow with the magnitude of 85 L/min (or 42.5 L/min if a dual-filter is employed). The selection of such flow rate is to reflect minute ventilation (minute volume) of breathing under high workloads. The penetration (ratio of downstream to upstream concentration) based on the mass median diameter (MMD) at 300 nm size measured with photometric

light scattering methods should be less than 5, 1 and 0.03 % for levels of 95, 99 and 100, respectively. The current certification only addresses the penetration through material media and does not include any relevance to the possible leakage pathways.

There are two major limitations associated with the certifications of NIOSH and 42 CFR 84 for utilization of the FFRs. First, NIOSH tests the filtration efficiencies at MMD of 300 nm, as this value represents the most penetrating particle size (MPPS) for mechanical filters. However various studies have shown the effect of electrostatic attraction of the charged media of the NIOSH-certified filters which dramatically shifts the MPPS towards nano-metric sizes (<100 nm) (Martin and Moyer, 2000, Balazy et al., 2006, Richardson et al., 2006, Eninger et al., 2008, Eshbaugh et al., 2009, Mostofi et al., 2011, 2012). With the second limitation, NIOSH's selected flow is a constant value (85 L/min), which may not fully represent the breathing flow, since the actual breathing resembles a cyclic pattern. Thus, it is highly necessary to investigate the performance of NIOSH-certified filters under cyclic flow rather than constant.

1.4 Thesis Objectives

Following to the limitations of previous works and certifications, this thesis pursues three main objectives introduced as below:

- Objective 1: Investigating the contribution of peak inhalation flow (PIF) and breathing frequency, in cyclic flows, on the penetration of poly-dispersed particles through one model of N95 FFRs;
- Objective 2: Investigating the penetration of poly-dispersed particles through one model of N95 FFRs under cyclic flows compared with constant flows equivalent to

the cyclic flow minute volume, mean inhalation flow (MIF) and peak inhalation flow (PIF).

- Objective 3: Investigation of poly-dispersed particle loading time effect on the efficiency of one model of N95 FFRs performed with constant and cyclic flow.

1.5 Thesis Overall Scope

Following the current chapter (introduction), chapter 2 will review the current literature corresponding to the particulate filtration by FFRs. Chapter 3 will describe the methodology and experimental design provided to complete this thesis. Results and analysis of each objective, accompanied by the discussions, will be given in chapter 4. Finally, the conclusions will be summarized and current limitations and future works will be addressed by chapter 5.

CHAPTER 2: LITERATURE REVIEWS

2.1 Particulate Filtration: Theoretical Approach

The use of FFRs is, in fact, employing the particulate filtration process to remove harmful particles from the inhaled air. The capability of filter material to efficiently capture the exposed particles depends on several factors varying from the physical and chemical essence of filtering material (i.e. filter chemical composition, filter thickness, fiber packing density, charge state of media etc) to the external exposure conditions (i.e. particle chemical composition, particle size, face velocity or air flow, steady or unsteady pattern of flow, charge state of particle, temperature, relative humidity, loading time etc). Each of these items can have minor or substantial impact on the efficiency of individual filtration mechanisms as well as filter overall efficiency. The filter overall efficiency is estimated by adding the impact of individual filtration mechanisms efficiency. Hence, as the first step, it is necessary to address the role of individual particulate filtration mechanisms.

2.1.1 Filtration Mechanisms

The particulate filtration is accomplished through four mechanisms (Hinds, 1990). Figure 2-1 provides the schematic approach for each of filtration mechanisms. These mechanisms are:

1- Inertial impaction;

2- Interception;

3- Diffusion; and

4- Electrostatic attraction

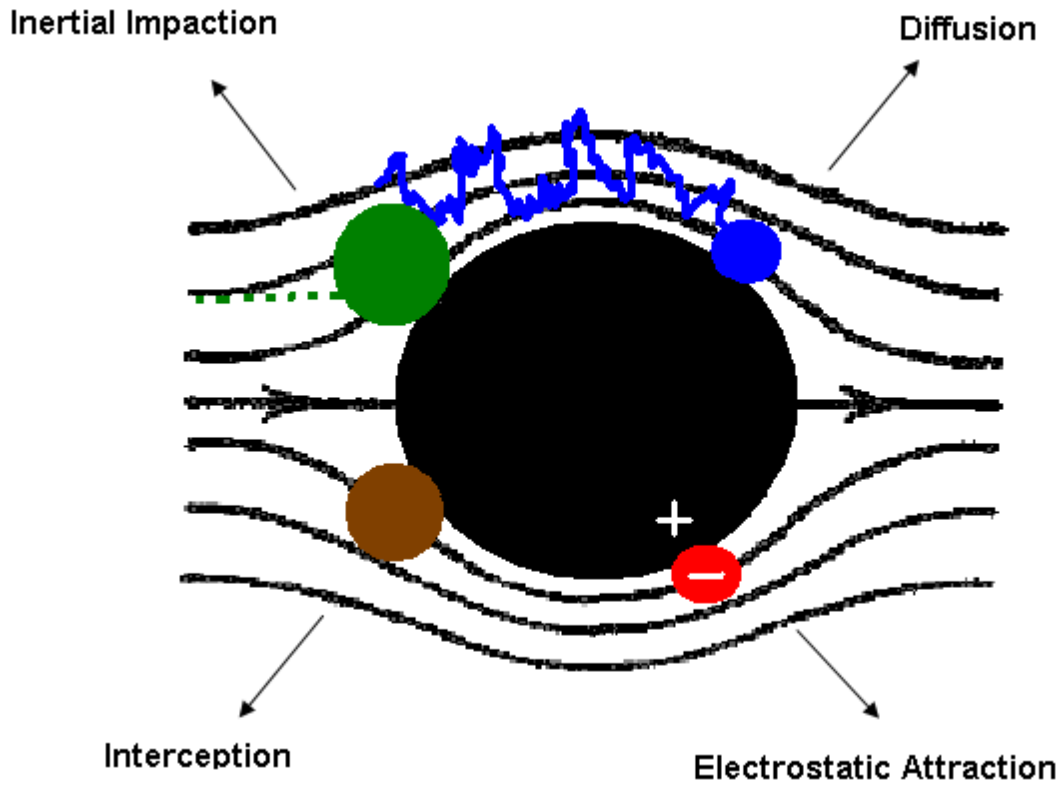

Figure 2-1: Particulate filtration mechanisms (Adapted from Haghighat et al., 2012)

Inertial impaction takes place when the particle inertia is too high that causes changing in the direction of particle motion in the airflow stream (Hinds, 1990). Particles with larger sizes, higher face velocities and densities have higher inertia, thus they are more easily captured by this mechanism. Overall, the particles with approximately 1 μm or larger can be effectively eliminated by this mechanism (Janssen, 2003). We can neglect the effect of this mechanism in capturing UFPs and NPs.

Interception takes place when a particle pursues its main streamline to come within one particle radius of the surface of a fiber (Hinds, 1990) making the contact between particle

and filter media. This mechanism is effective for removal of particles with large sizes down to 0.6 μm (Janssen, 2003). Interception is not mainly influenced by the velocity of particles, though it becomes more noticeable if particle size is increased. The major difference between interception and inertial impaction is that no deviation from the main streamline takes place with interception, but the particle is intercepted by the filter material.

Diffusion which is the most effective mechanism for capturing particles with sizes less than 0.2 μm occurs based on the random Brownian motion of particles bouncing into the filter media (Janssen, 2003). The irregular motion of particles, in fact, enhances the probability of collision between particles and fiber in a non-intercepting streamline (Hinds, 1990) which makes diffusion more significant rather than interception in capturing very small particles such as UFPs and NPs. As particle size or the face velocity is reduced, diffusion rate becomes more pronounced. With lower velocities, the particle residence time is increased through filter media; therefore the probability of collision between particle and filter media is highly increased.

The filtration devices removing the particles by means of the combination of inertial impaction, interception and diffusion are referred as mechanical filters in literature (Mostofi et al., 2010).

In order to increase the filter efficiency level, an additional mechanism called *electrostatic attraction* can be added to the filter by charging either media or particles. Electrostatic attraction mechanism is reduced by increasing velocity. The charged filters showing the electrostatic attraction in addition with the mechanical mechanisms

(diffusion, interception and inertial impaction) are so-called as “electrets filters” in literature (Brown et al., 1988, Fjeld and Owens, 1988, Janssen et al., 2003). Most of the NIOSH-approved filters (like N95 and P100) are known as the electrets filters.

2.1.2 Most Penetrating Particle Size (MPPS)

The overall filtration efficiency is estimated by combining the effect of all capturing mechanisms (impaction, interception, diffusion and electrostatic attraction). For sub-micrometer particles filtered by mechanical filters, interception and diffusion are the most dominant mechanisms, while inertial impaction is negligible. According to the behavior of latter mechanisms (diffusion and interception), in terms of particle size, presented by figure 2-2, the overall filtration efficiency is expected to be minimized at almost the intersection of two mechanisms in mechanical filters. This point is usually referred as the “Most Penetrating Particle Size (MPPS)” indicating the worst-case scenario size at which the penetration reaches its highest value (see figure 2-2).

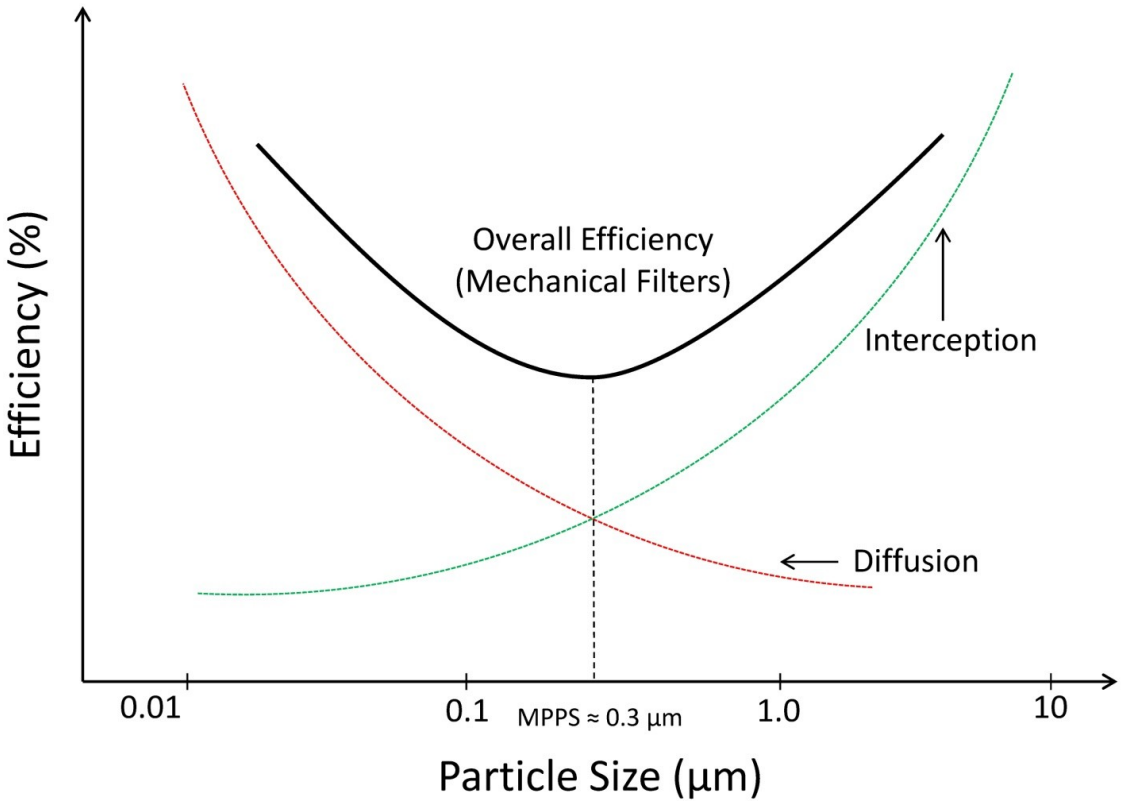

Figure 2-2: Most penetrating particle size (MPPS) in terms of interception and diffusion mechanisms

Based on the single fiber filtration theory, MPPS normally occurs at 300 nm for mechanical filters. The MPPS could be, however, subject to change. Supposing the diminishing effect of face velocity on diffusion and its inert effect on interception, the intersection of the two mechanisms could possibly take place at smaller sizes. Thus, the MPPS is expected to slightly shift towards smaller particles when the velocity is increased. For electrets filter, on the other hand, the presence of electrostatic attraction is expected, by theory, to significantly shift the MPPS towards smaller sizes compared to mechanical filters, since a new mechanism is added to diffusion and interception. In this regard, figure 2-3, indicates the overall efficiency and the occurrence of MPPS shifted towards nano-metric sizes, compared with mechanical filtration.

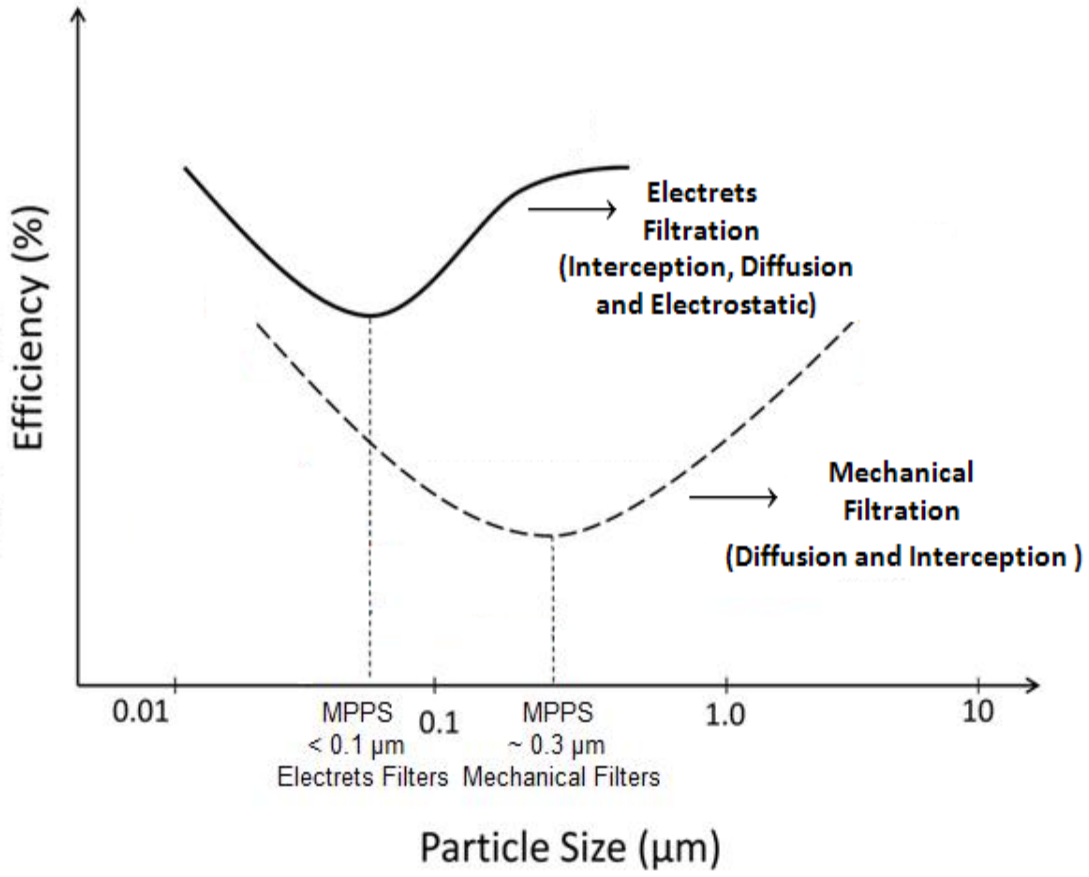

Figure 2-3: Most penetrating particle size (MPPS) for mechanical and electrets filters

2.2 Particulate Filtration: Experimental Approach

In support with the theoretical approach introduced in section 2.1, several experimental studies have surveyed the effect of influencing items on the filtration efficiency to make appropriate adjustments with the theoretical approach. The discussion about the experimental approach is classified through the charge, flow rate and loading effects which will be further discussed.

2.2.1 Charge Effects

The contribution of charge effects on overall filtration efficiency is the addition or strengthening of electrostatic attraction mechanism which can significantly increase the efficiency. Depending on the charge carried by the filter media, by the exposed particles or by both filter and particles, the filtration efficiency is subject to change. Several studies have investigated the effect of charged and neutralized filters (Martin and Moyer, 2000, Brown et al., 1988, Huang et al., 2007a, Janssen et al., 2003, Oh et al., 2000, Wang, 2001), while some other studies addressed the impact of charged particles on the FFRs performance (Balazy et al., 2006a, Kim et al., 2006). Similarly, some have investigated the effect of filter charge and particle charge at the same time (Chen and Huang, 1998, Fjeld and Owens, 1988, Yang and Lee, 2005, Yang et al., 2007). Combination of utilizing electrets filters with air ion emissions also lead to higher penetrations (Lee et al., 2005, Lee et al., 2004, Luo et al., 2009).

Presence of the electrostatic attraction mechanism in NIOSH-approved filters has been investigated by Martin and Moyer (2000). They measured the efficiency of three models of N95 and one model of each N99, R99 and P100 filters, under two conditions: as received (without treatment) and dipped in the iso-propanol (IPA) (for charge removal purposes). The maximum penetrations at MPPS were less than 5 % for N99 and N95, 0.03 % for R99 and 0.001 for P100 filters when the filters were not treated. However, for the case when the filters were dipped into the IPA, the maximum penetration changed to 33-55, 50 and 4 %, respectively (Martin and Moyer, 2000). The MPPS was drastically moved from 0.05-0.1 μm to 0.25-0.35. This indicated that the performance of N95, N99, R99 and P100 filters and the location of MPPS are highly related to the electrostatic

attractions (Martin and Moyer, 2000). Similarly, Janssen et al. (2003) measured the particle penetration through two different models of N95, R95 and P100 filters exposed to NaCl particles. Each filter was tested under three treatment conditions: untreated, exposed with irradiated ionization, and immersed with IPA. Their results showed the penetration was degraded by 0.561, 6.79 and 26.9 % for one N95 model for untreated, irradiated and IPA-dipped, respectively. Similar degradation rates were also observed with other filters (Janssen et al., 2003). Huang et al. (2007a) investigated the effect of removing charge for two models of electrets fibrous respirators (N95 and FFP1 (EN149:2001) mask) by dipping them into IPA for 5 minutes. The filters were exposed to poly-disperse 4.5 nm-10 μm NaCl aerosols. It was observed that the penetration could significantly rise for the sizes in 10 nm-5 μm. The maximum penetration were changed from 5.8 % to 18.9 % for "without treatment" and "treatment with IPA" situations, respectively (Huang et al., 2007a). Oh et al. (2002) compared the collection efficiency of conventional filters and electrets filters exposed by 0.5 μm NaCl particles and obtained a lower efficiency value for conventional filters. Similar results were obtained for the comparison of conventional filters (like dust-mist, (DM), dust-fume-mist (DFM) and surgical masks) to the electrets filter (like NIOSH-approved N95 filters (Balazy et al., 2006b, Qian et al., 1998). Brown et al. (1988) measured the penetration of urea aerosols on the charged and uncharged resin-wool and poly-carbonate materials and found considerably lower penetration curves (in terms of aerosols size) for charged fibers.

The impact of electrostatic attraction mechanism can also be detected by the particles charges. Charged particles results in the lower penetration (higher efficiency) compared to the neutralized particles. In this regard, Balazy et al. (2006a) measured the penetration

of poly-dispersed NaCl particles (10-200 nm) through N95 respirators under 85 L/min flow for two cases of charged and neutralized. The charged particles were shown to have more collections compared with the neutralized particles. Kim et al. (2006) measured the filtration efficiency of glass fibrous filters under exposure of 2 to 100 nm NaCl particles with 2.5 cm/s face velocity in three different particle charge states: uncharged particles, neutralized particle and charged particles. It was observed that filtration efficiency is the least for uncharged particles, but most for charged particles.

The filtration efficiency can be doubly enhanced by the simultaneous impact of charged media and charged particles. Chen and Huang (1998) measured the penetration of mono-disperse corn-oil particles for four sizes of 1, 1.6, 2.2 and 2.5 μm for electrets and IPA treated filters as a function of particle charge number carried by particle under 10 cm/s face velocity. The results illustrated that, for all sizes, electrets filter with the most tested charge number (1200 n) had the lowest penetration. Inversely, treated filters being exposed to no charged particle represented highest penetration (Chen and Huang, 1998). Fjeld and Owens (1988) investigated the effect of 0.5 μm polystyrene aerosol penetration in terms of particle charge under 1 cm/s face velocity. Original electrets filters and discharged filters were tested during this experiment. Results indicated a descendent curve for penetration in terms of particle charge for both the original and discharged filters indicating the penetration decreases when the charge is added to the particle. On the other hand, the original filters (representing electrets) showed lower penetration compared with the discharged ones (Fjeld and Owens, 1988).

Ion emission was found to be a significant impact on particle penetrations. Lee et al. (2004) investigated the effect of unipolar ion emission on the particle penetration through

N95 respirators and surgical masks. Particles were within the range of 0.04-0.5 μm. The results indicated significantly higher penetration for the respirators without ion emission effect. As particles were exposed by the ion emission for more time, the penetration curve versus particle size was reduced. These conclusions were consistent with a later work done by the same researchers for other types of respirators such as dust-mist (DM) and R95 (Lee et al., 2005). Luo et al. (2009) investigated the effect of negative air ion (NAI) emission (in three different emission rates) on the performance of electrets filters for removal of two bioaerosol types: E-coli and Bacillus subtilis endospores. The reduction in penetration was proportional to the rate of emission, indicating positive effect of ionized aerosols on filter efficiency (Luo et al., 2009).

2.2.2 Flow Effects

The impact of flow rate has been also widely discussed, since higher flow rate is associated with higher inhalations, which could potentially vary the filtration efficiency. The discussion about the impact of flow rates covers both constant and cyclic flow. Constant flows are mostly selected in order to adapt the test criteria to the standard and regulations (85 L/min according to 42 CFR 84, 1995). Cyclic flow selections, on the other hand, reflect the actual breathing flow in human which follows a cyclic pattern rather than the constant. These items will be reviewed, in separate.

2.2.2.1 Impact of Constant Flows

Increasing flow rate (or face velocity) can significantly increase particle penetration through filter media. Such penetration increase is mainly due to the reduction of the efficiency of the electrostatic and diffusion mechanisms (Janssen, 2003, Hinds, 1990). Several studies have widely observed that the enhanced flow rate causes a distinct increase in penetration (or reduction in filtration efficiency) (Kim et al., 2007; Steffens and Coury, 2007; Boskovica et al., 2008, Chen and Huang, 1998, Yang and Lee, 2005, Huang et al., 2007a, Huang et al., 2007b, Yang et al., 2007, Stevens and Moyer, 1989; Fardi and Liu, 1991; Chen et al., 1992; Hanley and Foarde, 2003; Qian et al., 1998; Balazy et al., 2006a,b; Eninger et al., 2008; Rengasamy et al., 2008; Mostofi et al., 2011).

Qian et al. (1998) measured the efficiency of N95 and three conventional DM, DFM and surgical masks under 32 and 85 L/min flow rates. The test was performed by generation of mono-disperse NaCl aerosols ranging from 0.1 to 0.6 um and mono-disperse PSL ranging from 0.6 to 5.1 μm. They observed lower efficiency values for all filters under the constant flow rate of 85 L/min compared to 32 L/min. Balazy et al. (2006a) tested two N95 models under 30 and 85 L/min flow rate selections exposed by poly-disperse NaCl particles within 0.01-0.6 μm. They observed significantly higher penetrations for several sizes between 0.02 and 0.1 μm for both models. Other similar tests by Balazy et al. 2006b showed the same trend for bio-aerosols such as MS2 viruses (in range of 10 to 80 nm) under the same flow rates (30 and 85 L/min) for N95 and surgical masks (Balazy et al. 2006a). Huang et al. (2007a) measured the effect of air flow rate on the IPA treated FFP1 (EN149:2001) fibrous filter under 30, 60 and 85 L/min using 4.5 nm-10 μm NaCl aerosols and reached the same result as previous research. For example at 300 nm, the

penetration for 30, 60 and 85 L/min were reported as 47, 66 and 79%, respectively. Eninger et al. 2008 measured the penetration of NaCl particles, MS2, B Subtilis phage and T4 phage bio-aerosols (poly-dispersed) through one model of N95 and two models of N99 respirators, for the range of 0.02-0.5 μm, under 30, 85 and 150 L/min. The maximum penetration of NaCl particles was measured as 8.1, 4.8 and 1.4 % for 150, 85 and 30 L/min, respectively for N95. For the first model of N99 such penetrations reached 10.2, 5.9 and 1.3 %, respectively; and for the second model of N99 these numbers were recorded as 6.6, 4.3 and 1 %, respectively. The MPPS for all flow rates was found at 30-70 nm with a slight tendency towards the smaller sizes at high flow rates. Mostofi et al. 2011 investigated the impact of increased air flow rate (85, 135, 270 and 360 L/min) by exposing a model of N95 to 15-200 nm poly-disperse NaCl particles. The maximum penetrations (at MPPS) reached 2.7, 6.6, 11.7 and 15.3 % for the tested flow rate, respectively. The MPPS was also observed to be dislocated from 46 to 36 nm from 85 to 360 L/min.

2.2.2.2 Impact of Cyclic Flow

Rather than the constant flow, the impact of cyclic flow rate on the particle penetration has also been studied (Jordan and Silverman, 1961, Stafford et al., 1973, Brosseau et al., 1990, Richardson et al., 2006, Haruta et al., 2008, Cho et al., 2010, Grinshpun et al., 2009, Eshbaugh et al., 2009, Rengasamy et al., 2011a,b, 2012, Wang et al., 2012, He et al., 2013a,b, Gardner et al., 2013). Among these studies, few studies particularly addressed the comparison of penetrations measured between the cyclic and constant flows (to establish an appropriate adjustment between the certification protocol and the real workplace conditions). The penetrations under cyclic flow were typically compared

with the penetrations measured under constant flows equal to the minute volume, mean inhalation flow (MIF) and peak inhalation flow (PIF) of the cyclic flows (see figure 2-4). Minute volume is defined as the average amount of air flow inhaled per one minute of breathing, while mean inhalation flow (MIF) is characterized by the amount of total volume of the air flow inhaled in one inhalation cyclic divided by the inhalation cycle period. Peak inhalation flow (PIF) is the maximum flow obtained in one inhalation cyclic. For a sinusoidal flow (as selected for all cyclic flows in this study), it is proven that, regardless of the breathing frequency, the PIF is π times as the minute volume and π/2 times as MIF.

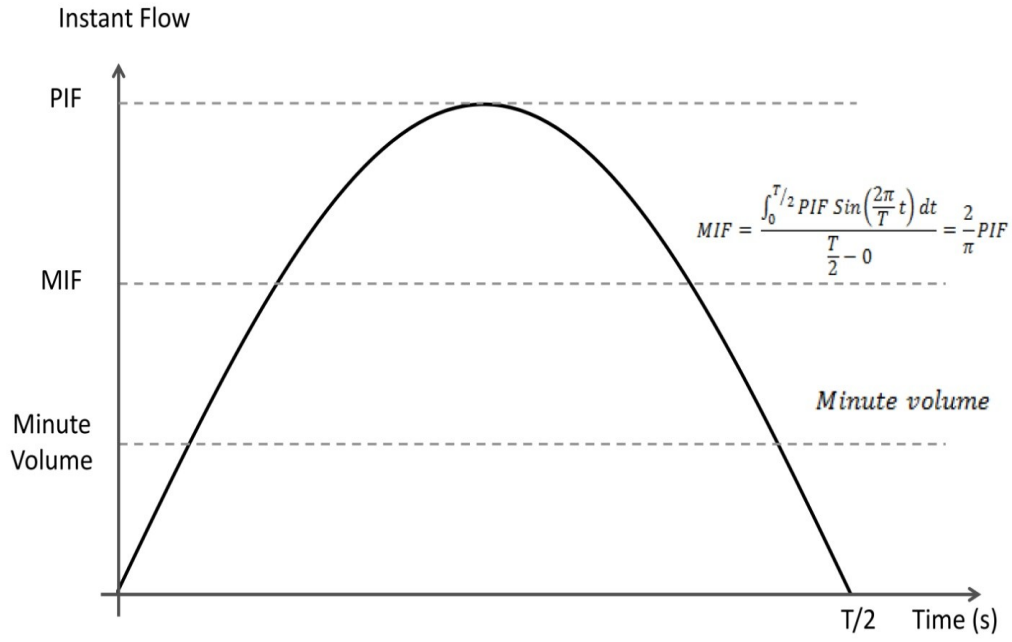

Figure 2-4: Scheme of cyclic flow and constant flows equal to cyclic flow minute volume, mean inhalation flow (MIF) and peak inhalation flow (PIF); T/2 is considered as inhalation cycle period

Jordan and Silverman (1961) measured the aerosol penetration (0.78 μm as count median diameter (CMD) and 1.13 as geometric standard deviation (GSD)) through fiberglass

filters under the cyclic flows using low and high time-average face velocities. It was concluded that the cyclic flows with high time-average face velocities have higher penetrations. Stafford et al. (1973) tested performance of three models of respirator filter cartridges by comparing the impact of three cyclic flows with the MIFs of 30, 35 and 53 L/min and a constant flow of 32 L/min on the penetration of mono-disperse poly-styrene latex (PSL) and dioctyl phthalate (DOP) particles. The PSL and DOP particle size selected were 0.176-2.02 μm and 0.3 μm, respectively. Brosseau et al. (1990) also investigated the penetration of silica (0.46 μm) and asbestos (4.5 μm as length and 0.2 μm as width) particles on the DM filters under cyclic flows with equivalent peak inhalation flow (PIF) of 100 L/min and mean inhalation flow (MIF) of 76 L/min compared with constant flow of 32 L/min. The results of both latter studies indicated that the penetration measured with the cyclic flow was typically higher than the penetration obtained by the constant flow.

Richardson et al. (2006) and Eshbaugh et al. (2009) evaluated the performance of N95 and P100 FFRs and cartridges challenged by 0.02-2.7 nm particles. N-series filters were challenged by NaCl (0.02-0.3 μm) and PSL (0.7-2.9 μm), while P-series filters were challenged with DOP (0.02-0.3 μm) and poly-alpha olefin oil (0.7-2.9 μm). Filters were tested under three constant flows with the rates of 85, 270 and 360 L/min and cyclic flows with rates of 40, 85, 115 and 135 as minute volume (or 135, 270, 360 and 430 L/min as PIF, respectively). It was concluded that, a constant flow equal to the MIF or PIF of the cyclic flow could better predict the penetration under the cyclic flow (Richardson et al., 2006, Eshbaugh et al., 2009). Their results showed that penetrations were higher with cyclic flows, when they were tested with the constant flow of 85 L/min

and the cyclic flow with the same value as minute volume (equal to 270 L/min as PIF). It was also indicated that the cyclic flows tended to cause a slight increase in penetration, when constant flows with rates of 85 and 270 L/min and the cyclic flows with the same values as MIF were compared. Unlike minute volume and MIF, the penetration under constant flows of 270 and 360 L/min was slightly higher than the cyclic flow with same values as PIF (Richardson et al., 2006, Eshbaugh et al., 2009). Haruta et al. (2008) assessed the effect of constant flows with rates of 15, 30, 85 and 135 L/min and cyclic flows with the equivalent MIFs. The tests were performed with for the PSL UFPs possessing the effective sizes of 25, 65 and 99 nm (GSD<1.1; mono-disperse). Consistent to the results of Richardson et al. 2006, the magnitude of penetration was found to be higher with cyclic flow than the constant flow for the first two constant-cyclic couples (15 and 30 L/min). However, almost similar values were recorded for the penetration measured under constant and cyclic flows with a rate of 85 L/min. For the highest flow selection (135 L/min), the penetration under the constant flow was higher compared with the penetrations measured by the cyclic flow. Wang et al. 2012 compared the penetration of N95 and P95 dual-filter cartridges obtained by the constant flow ranging from 32 to 320 L/min and the cyclic flows with equivalent minute volumes ranging from 16 to 130 L/min when they were challenged with PSL particles (0.3 μm) on. Similar to results of Richardson et al. (2006) and Eshbaugh et al. (2009), the penetration obtained under cyclic flow was more than the penetrations measured with the constant flow equivalent to minute volume and MIF, but less than the penetrations measured under constant flow with equivalent to PIF. Rather than the comparison between constant and cyclic flow, Wang et al. (2012) measured the penetration of 0.3 μm polystyrene latex (PSL) particles

through N95 and P95 cartridges with dual-filter elastomeric half-face masks, under various cyclic flows with the same equivalent minute ventilation (minute volume of the cyclic flow) of 50 L/min but different patterns, including two sinusoidal, one trapezoidal and one exponential. They observed higher penetration values with the exponential cyclic flow (which had higher peak inhalation flow (PIF)), almost the same values for two sinusoidal flows (which had the same PIF but different frequencies and tidal volumes), and lower for the trapezoidal flow (which had the lowest PIF). Additionally, the constant minute volume flow led to the lowest penetration compared to all the selected cyclic flows. In a recent study, Gardner et al. (2013) investigated the effect of constant and cyclic flows on the penetration of inert aerosol (NaCl, 50 nm) and MS2 viruses (500 nm as MMD) on N95 and P100 FFR and cartridges, for two constant flow rates (85 and 270 L/mina) and two cyclic flow rates (85 and 135 L/min as minute volumes). They found that all N95 and P100 filters efficiencies met or exceeded the capturing efficiency of MS2 viruses for whether low or high flow rates. The comparison between the constant and cyclic flows penetration also indicated that, a constant flow equal to MIF or PIF of the cyclic flow would better represent the cyclic flow penetration.

2.2.3 Particle Loading Effect

In general, for mechanical filters, the loading effect comes with the increase in filtration efficiency as well as the increase in pressure drop (Leung and Hung 2008, 2012). Leung and Hung (2012) also observed that, the MPPS shifts towards smaller sizes due to the agglomerated particles improving the efficiency by diffusion and interception mechanism with a more prominent way in interception. For electrets filters, on the other hand, the penetration is firstly increased (efficiency is decreased), since electrostatic attraction

forces are covered by deposited particles. Such an increase in penetration is then followed by a reverse trend (decrease in penetration) after a certain particle deposit, since the filter could behave like a mechanical filter (Brown et al., 1988, Barret and Rosseau, 1998, Wang, 2001).

Investigations of loading effect on NIOSH-approved filters have been, however, very limited (Barret and Rosseau, 1998, Moyer and Bergman, 2000, Mostofi et al., 2011). Barret and Rosseau (1998) tested advanced electret filter media (materials prepared for NIOSH-approved filters: N, R and P series) with loading of NaCl (0.08 μm as count median diameter (CMD) and 0.2 μm as MMD) and DOP (0.18 μm as CMD and 0.3 μm as MMD) under 85 L/min constant flow, up to 200 mg challenge aerosol load. They found out that the penetration and pressure drop were initially increased with the aerosol challenge load. However, the loading penetration of advanced electrets filters was found to be 10 fold smaller than the loading penetrations obtained for conventional electrostatically charged blown microfiber media (with the same pressure drop for both filter materials). Moyer and Bergman (2000) determined the loading effect of small masses of NaCl (count median diameter (CMD) of 75 nm with geometric standard deviation (GSD) of less than 1.82) for a challenge concentration of typically 5 ± 1 mg/day on N95 filters, under 85 L/min constant flow rate. The loading tests were performed for a period of one day and were repeated once in a week for a period of weeks. Between two consecutive testing periods, the N95 filters were kept uncovered, outside the test laboratory, without exposure to NaCl particles. The results showed that, within a one-day period (in each single week), the particle penetrations were decreased with the loading time. However, between the consecutive periods (from one week to the

next week) an increase in the average penetration was observed. Mostofi et al. (2011) investigated the loading effect of poly-dispersed NaCl particles (ranging from 15 to 200 nm) on N95 FFRs for a period of 5 hours under 85 L/min flow. The results indicated that a significant decrease in penetration occurred for particles with sizes less than 100 nm. The average penetration for nano-metric sizes was, for instance, reduced from 1.76 to 0.87 % for the initial and final stage of loading, respectively. However, for larger particles the penetration slightly increased with the exposure time. The final average penetrations for 100-200 nm were recorded as 1.07 % compared with the initial penetration of 0.71 %. The MPPS was also observed to be significantly shifted from 41 to 66 nm for initial and final stages, respectively.

2.3 Study Limitations and Objective Selection

Although several information about the performance of FFRs for particle removal is available in the literature, there are various aspects that have been, by now, undocumented. The undocumented items will be classified into sections 2.3.1 and 2.3.2, 2.3.3 separately, to address the objectives of this thesis.

2.3.1 Objective 1

None of the earlier studies investigated the individual contribution of breathing frequency and PIF on penetration, specifically at the nano-size ranges (<100 nm). Unlike the constant flow, which is characterized by only one parameter (magnitude of constant flow), the cyclic flow is characterized by two parameters: breathing frequency and peak inhalation flow (PIF). Considering that breathing frequency and inhalation flow rate simultaneously increase from sedentary to heavy workloads in a real respiratory process

(Blackie et al., 1991; Carreti et al., 2004; Janssen et al., 2005; Anderson et al., 2006), penetration variations could be attributed to the rise in both flow and frequency; thus, it is necessary to investigate the individual contribution of each parameter. In addition, there are differences in the literature about the experimental setups used. Some of the earlier studies ignored the exhalation cycles and only considered the inhalation portion (Haruta et al., 2008; Eshbaugh et al., 2009 (sub-micrometer test apparatus); Grinshpun et al., 2009; Wang et al., 2012); however, other studies considered both inhalation and exhalation flows (Eshbaugh et al., 2009; Cho et al., 2010; Rengasamy and Eimer, 2011, 2012, He et al., 2013a,b).

The first objective of this thesis is the development of a procedure to investigate the individual impact of breathing frequency and flow rate on the performance of one model of N95 FFR. The study was performed using two different experimental setups (only inhalation, and both inhalation and exhalation).

2.3.2 Objective 2

Summarizing the results from previous works gives useful information regarding the performance of N95 filters under cyclic flows and the comparison with constant flows. Nonetheless the information, available in literature, is limited due to two reasons: First, there is no general agreement in the literature on the impact of cyclic and constant flows on the penetration. This is mainly due to the diversities in experimental setups, type of filter materials and type of challenge particles utilized. Second, no earlier study investigated the effect of poly-dispersed particle penetration under the cyclic flow and the information is limited only to mono-disperse particles. Therefore, it is necessary to

measure the penetrations of poly-disperse particles under the cyclic flow. Poly-disperse particles reflect a more realistic situation.

The second objective of this thesis is to address the impact of poly-dispersed particles penetration (mostly ultra-fine range; <100 nm) under cyclic flows and compare it with the penetrations obtained under constant flows equivalent to the minute volume, MIF and PIF of the cyclic flow.

2.3.3 Objective 3

Summarizing the results from previous works reveals that, the effect of loading time for poly-dispersed particles, on the performance of N95 filters has been discussed by only one previously peer-reviewed paper (Mostofi et al., 2011). Nonetheless the selection of the latter study was limited to only a single constant flow. The third objective of this thesis is to evaluate the efficiency of N95 filters under both constant and cyclic flow (with minute volume of 85 L/min). Comparison tests between constant and cyclic flows are also performed in terms of initial penetration and the penetration associated with the loading time.

CHAPTER 3: MATERIALS AND METHODS

3.1 Experimental Design

3.1.1 Setup Configurations

Figure 3-1 illustrates the experimental setup used in this study (Mahdavi et al., 2013). The setup comprised of an experimental chamber, a manikin head, particle generation system, a breathing flow simulator, and measurement devices. Manikin-based system has been used in several earlier studies (Balazy et al., 2006a; Eninger et al., 2008; Rengasamy and Eimer, 2011a, 2012; Mostofi et al., 2011).

Figures 3-1a and 3-1b indicate the setups where cyclic flows were performed. With these setups, the manikin was connected to a flow/volume simulator (Series 1120; Hans Rudolph Inc., Shawnee, KS, USA) for creation of cyclic flows. Figure 3-1a shows the approach in which the exhalation flow was returned to the chamber simulating the actual breathing condition (setup 1: both inhalation and exhalation). Figure 3-1b illustrates that the exhalation flow was exhausted to the outside of the chamber using a three-way pressure valve (setup 2: only inhalation). As seen, an extra fan was placed for the first setup (figure 3-1a) to stabilize the concentration variations caused by the exhalation flow returning through the chamber. Figure 3-1c shows the constant flow setup. In this setup the outlet flow was directly used to draw the constant flow through the manikin head.

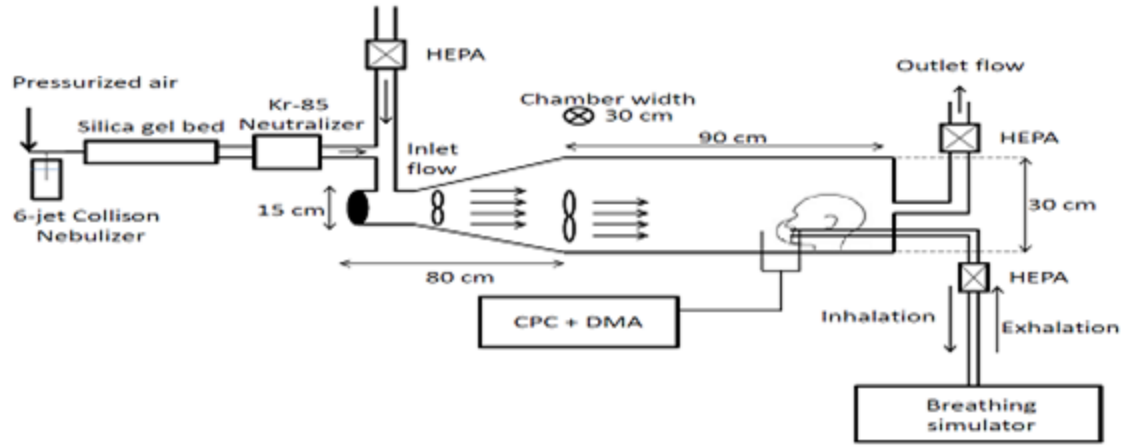

(a)

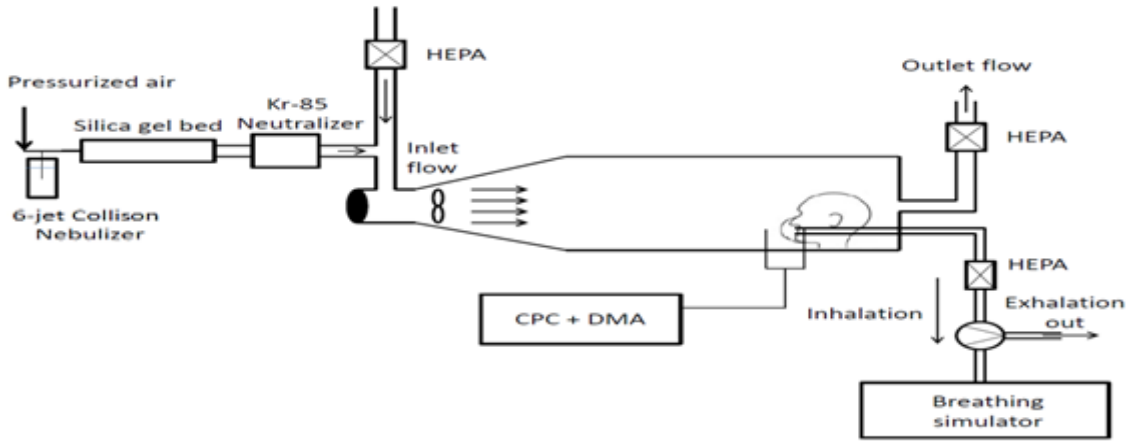

(b)

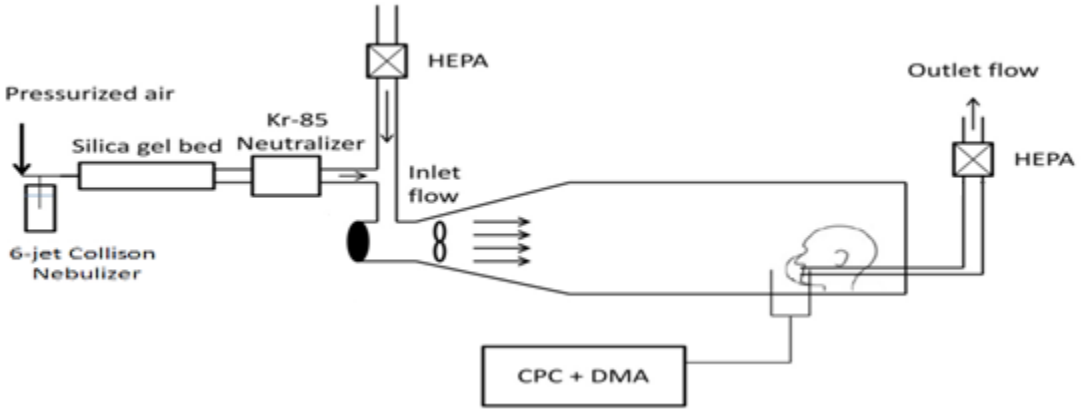

(c)

Figure 3-1: a) Experimental setup for cyclic flow (inhalation and exhalation); b) Experimental setup for cyclic flow (Inhalation only); c) Experimental setup for constant flow

3.1.2 Particle Generation System

Using a six-jet Collison nebulizer (CN 2425, BGI Inc., Waltham, MA, USA), containing 0.1% v/v NaCl solution, and a filtered air supply (Model 3074B, TSI Inc., Shoreview, MN, USA), the aerosol flow was provided under 30 psi pressure to generate 10–205.4 nm NaCl particles (see figure 3-2). Afterwards, the flow was passed through the drying system (silica gel packs) to control the humidity of the chamber (see figure 3-3). A Kr-85 electrostatic neutralizer (Model 3012/3012A, TSI Inc., Shoreview, MN, USA) was set to remove electrostatic charges carried by the generated particles (see figure 3-4). As discussed in literature, charged particles could significantly increase the filtration efficiency and not represent the worst-case particle penetration measurement (Yang and Lee, 2005; Balazy et al., 2006a; Kim et al., 2006). The aerosol flow was then diluted by the clean air and dispersed through the chamber. An outlet flow with a regulatory valve was used to balance the pressure in the chamber.

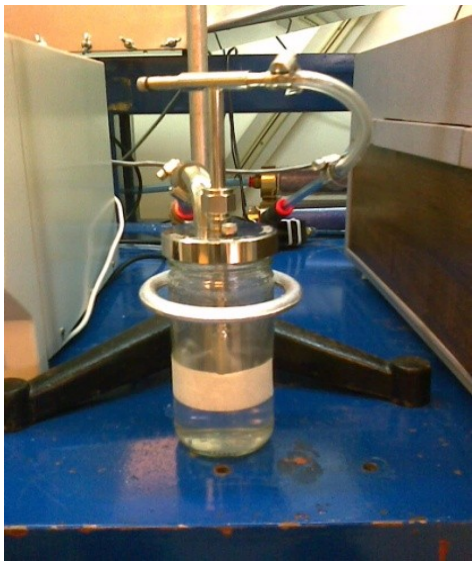

Figure 3-2: Generation system: 6-jet Collison Nebulizer

Figure 3-3: Generation system: drying system (silica gel bed)

Figure 3-4: Generation system: Kr-85 electrostatic neutralizer

3.1.3 Measurement Devices

A set of an "electrostatic classifier (EC)" (Model 3080, TSI Inc., Shoreview, MN, USA) containing a long DMA (differential mobility analyzer) and a "condensation particle counter (CPC)" (Model 3775, TSI Inc., Shoreview, MN, USA) was used to measure upstream and downstream concentrations distribution whether for constant or cyclic flow tests (see figure 3-5). For a given sample, the DMA classified particles within a certain size range based on their electric mobility diameter. Classified particles were then counted and recorded by the CPC. The technique of concentration measurement through

classifying (by DMA) and counting (by CPC) is also referred as scanning mobility particle sizer (SMPS) spectrometry. In each sample, the SMPS data for the tested size range (10–205.4 nm) was divided into 21 size channels. For each experiment, the downstream sample was completed first, then the sample probe was switched to upstream. The samples contained two scans from downstream and two scans from upstream (n=2), each with length of 180 seconds. After each scan, a 15-second retrace time was given by the device for DMA voltage adjustment, previous air sample clearance and preparation for the new scan. Therefore, the total sampling time (regardless of retrace times) for either downstream or upstream concentration was 360 seconds (180 times two), which, for cyclic flows, provided at least a 17-second time interval (360 seconds per 21 channel) for recording the concentration of each channel (size).

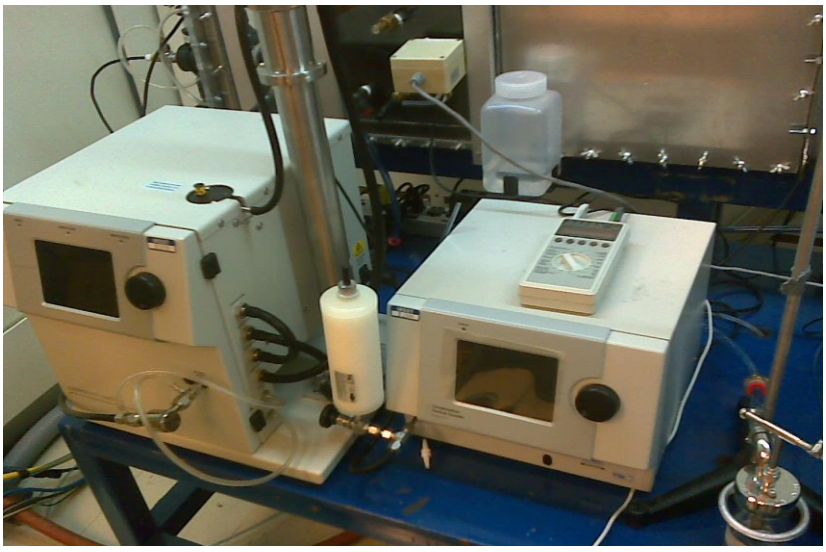

Figure 3-5: Electrostatic classifier (EC) (left) and condensation particle counter (CPC) (right)

3.2 Penetration Measurement

The particle penetration is defined as the ratio of two concentration distributions:

$$P(\%) = \frac{\left(\frac{dC}{d\log D_p}\right)_d}{\left(\frac{dC}{d\log D_p}\right)_u} * 100\% \qquad (1)$$

C and D_p indicate the number concentration and the particle diameter, respectively; thus the term (dC/d log D_p) represents the number concentration distribution in terms of particle size (#/cm^3). Subscripts *d* and *u* indicate the filter downstream and upstream, respectively.

3.3 Measurement Challenges with Cyclic Flow

As previously discussed, penetration is significantly influenced by the flow rate, therefore it is expected that the instant penetration is subject to vary during the cyclic flow (where instant flow rates vary in different times). For instance, we can assume that, the same as the cyclic flow, instant penetration reaches to a maximum level from zero; then it goes to zero level throughout an inhalation cycle.

The utilized method to measure the penetration is, as previously mentioned, SMPS spectrometry, since it is an appropriate method for recording poly-dispersed particles (where concentration has a distribution function). Despite, SMPS cannot record instant concentrations in terms of particle size. In fact, SMPS records the concentration (and penetration) of each size channel as an average value over a certain period of time (which is part of a whole SMPS sampling time). To make sure that the given time for SMPS (360 s) provides sufficient time to cover enough flow cycles per each channel, the penetration measured by SMPS mode is compared with another mode referred as “count” mode in

this study. With the count mode, the DMA voltage is set to a constant value to classify only one size of particles (unlike SMPS mode where the DMA voltage is varying in order to record concentration distribution ($dC/d\log D_p$)). The advantage of this mode is that the sampling can be adjusted for any desirable time (however the particle counts are recorded for one single size, only). The time intervals can be adjusted down to 0.1 second within the whole sample time, to almost estimate the instant counts measurements.

The verifications between two modes were made for two cyclic flows (with PIFs of 135 and 360 L/min) and two experimental setups (setup 1: inhalation and exhalation, and setup 2: inhalation only). For the count mode, three single sizes of 22.1, 39.2 and 107.5 nm were selected by the count mode and the downstream and upstream concentrations were measured. For each size at each stream (whether upstream or downstream) a certain period of 2 minutes was given to record an average value for concentration (the total of 6 minutes for all three sizes). For SMPS mode, as previously mentioned, a total period of 360 s (including two 180 s scan) was given for each upstream or downstream (for the range of 10-205.4 nm). For each flow rate, the penetration by both count and SMPS mode was accomplished for one single respirator. The penetrations were then compared to each other and the deviations between them were assessed (see figures 3-6 to 3-9).

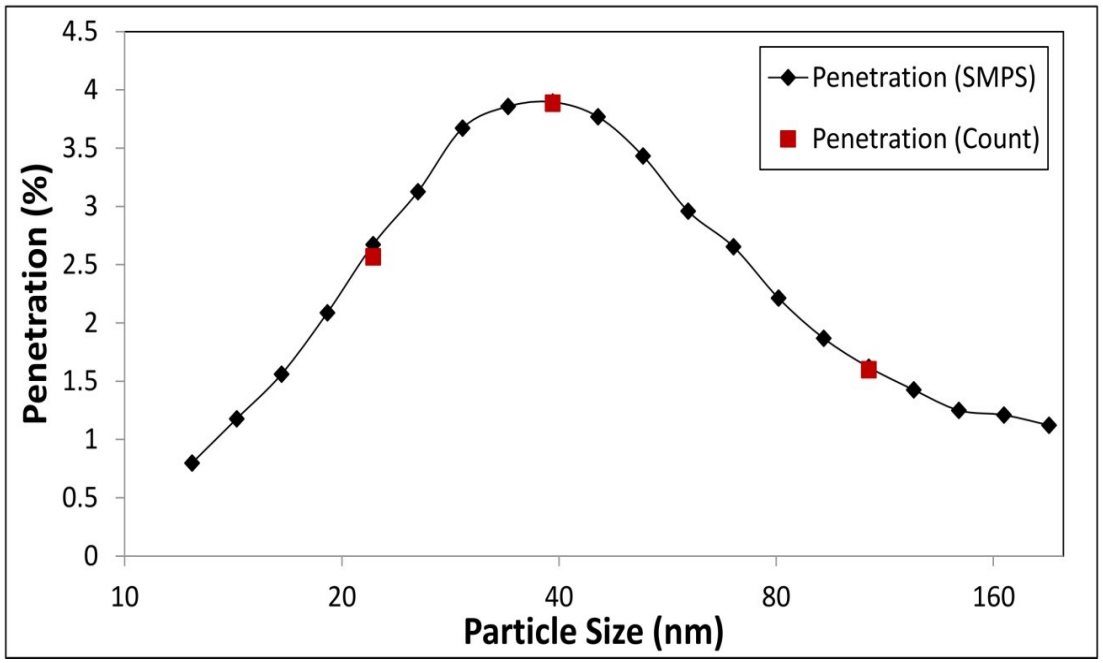

Figure 3-6: Penetration (SMPS) vs. Penetration (count) for cyclic flow rate of 135 L/min as PIF (inhalation and exhalation (setup1))

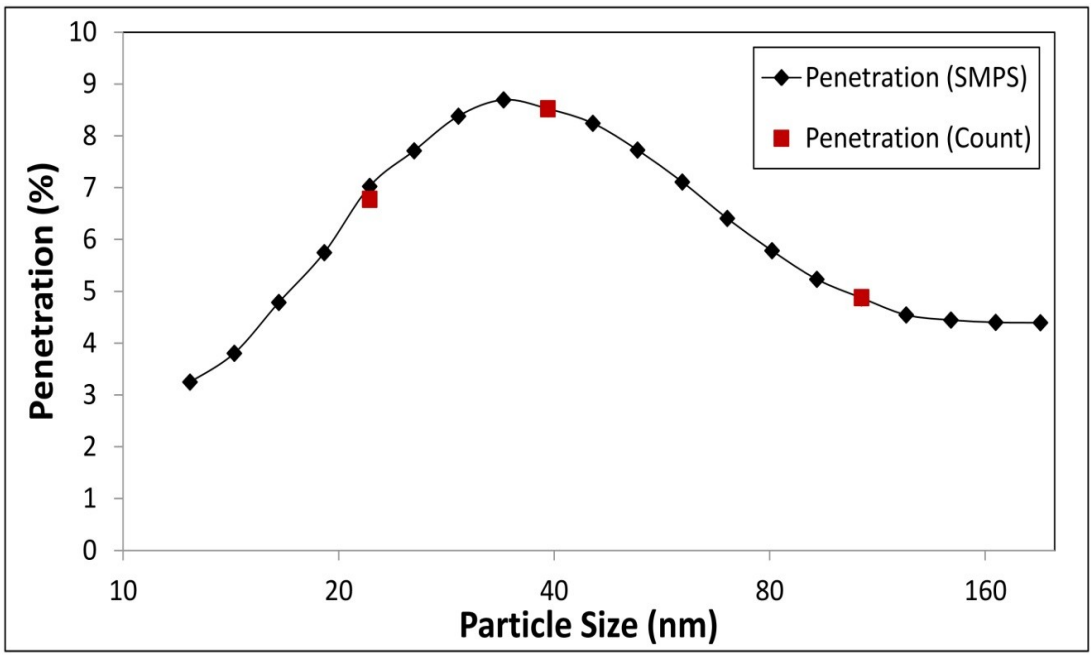

Figure 3-7: Penetration (SMPS) vs. Penetration (count) for cyclic flow rate of 360 L/min as PIF (Inhalation and exhalation (setup1))

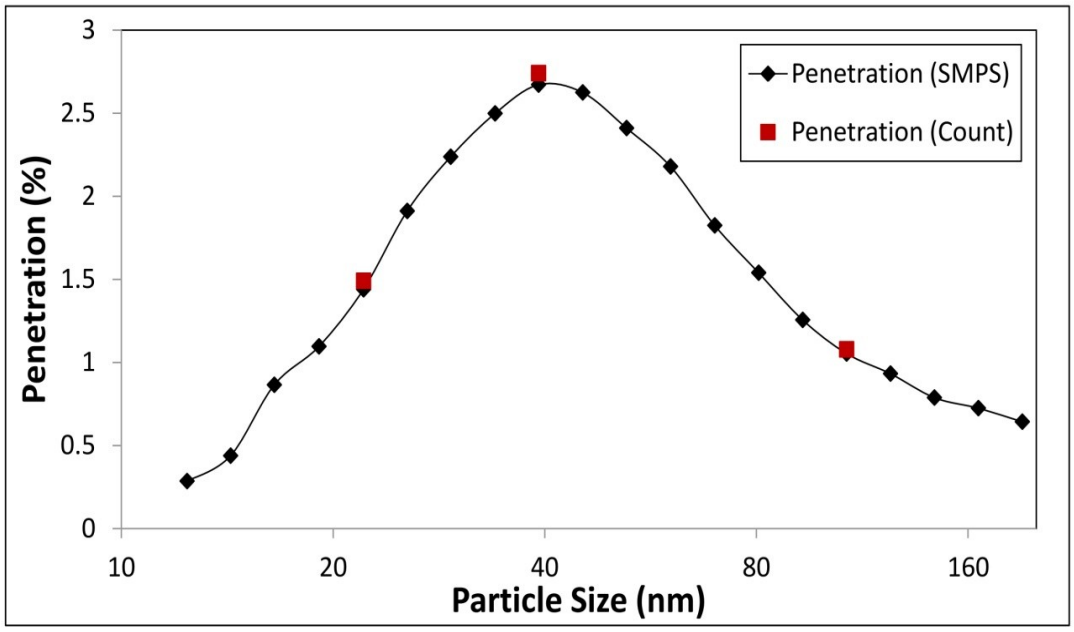

Figure 3-8: Penetration (SMPS) vs. Penetration (count) for cyclic flow rate of 135 L/min as PIF (inhalation only (setup2))

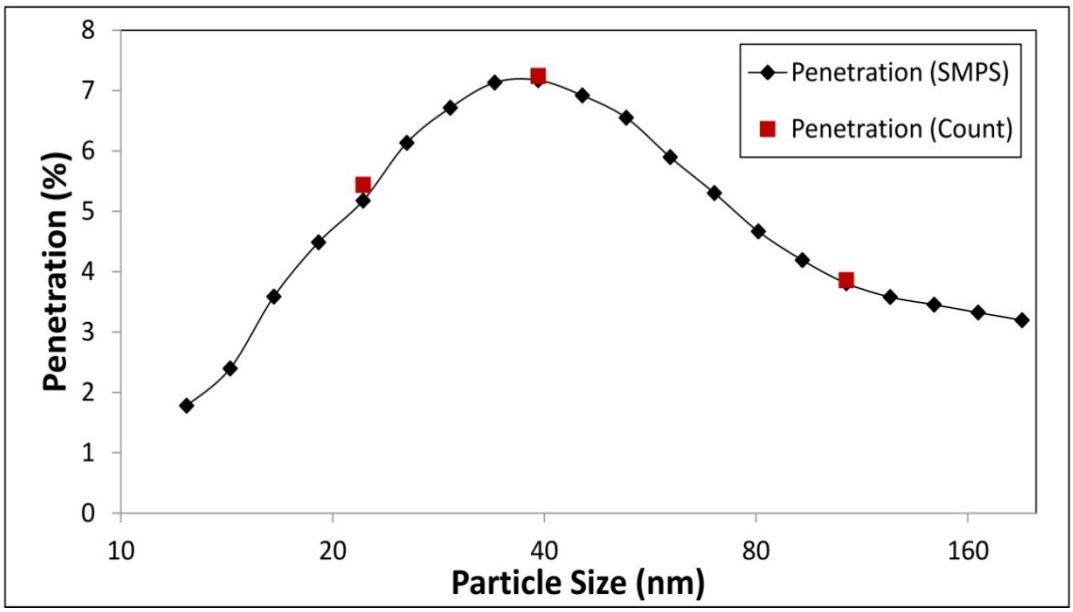

Figure 3-9: Penetration (SMPS) vs. Penetration (count) for cyclic flow rate of 360 L/min as PIF (inhalation only (setup2))

As seen in figures 3-6 to 3-9, the values for penetrations obtained by count and SMPS were close to each other. For the cyclic flow with 135 L/min under the first setup (inhalation and exhalation), for instance, the deviation between count mode and SMPS mode samples were 3.93, 0.26 and 1.3 % for the sizes of 22.1, 39.2 and 107.5 nm, respectively. Similarly, for all other flow rates the deviations between samples (count and SMPS) were found to be negligible. This validated that, for our flow selections, the selected sampling time (360 s) for SMPS is appropriate to obtain accurate average values (based on the time given) for penetrations measurement.

3.4 Setup Verification Tests

To ensure measurement accuracy, two verification test series were performed: “no-filter” and “stability: tests. With the no-filter tests, experiments were carried out with the manikin head without N95 FFR (“no filter” test) to check the uniformity of upstream and downstream concentration. The deviation between two samples throughout all size channels was then evaluated. With the stability test (after the concentration reached a stable value), upstream concentrations at times 0, 15, 30, 45 and 60 minutes were measured for all the selected flow rates, and the deviation among the samples throughout all size channels were assessed in order to check the upstream concentration remained stable, once the setup was run. In all cases, the maximum and the average deviation did not exceed 13 % and 5%, respectively. The maximum deviation in both verification tests normally occurred at the smallest or largest size channels (close to 10 or 205.4 nm, the two extreme sides) where the concentration distribution (in terms of particle size) was too low, compared to other size channels. However the deviations among channel concentrations in most of size channels (including the most penetrating particle size

(MPPS), as the worst-case scenario penetration measurement) were significantly less than the maximum deviation.

3.5 Respirator Selection

One model of cup-shaped N95 FFR (3M, Model 8210) was considered for the experiments of this study (see figure 3-10). The respirators were not preconditioned and they were tested, as received. After each test, the used respirator was taken off from the manikin and discarded and a new respirator was set for the next test. Each respirator was suitably sealed to the manikin by a silicone sealant to avoid leakage. Therefore this study does not address the leakage pathways for penetration of UFPs.

Figure 3-10: N95 FFR, 3M, model 8210

3.6 Procedure for Objective 1

3.6.1 Parameters: Enhancement Fraction Values

For a given size and filter, the magnitude of penetration under a sinusoidal cyclic flow is a function of breathing frequency (Fr) and PIF, assuming all other influencing

parameters (such as humidity, temperature, loading time and loaded mass) are constant. One can write

$$P = f(PIF, Fr) \tag{2}$$

In such a scenario, the variations in penetration due to PIF and Fr can mathematically be expressed as:

$$dP = \left(\frac{\partial P}{\partial PIF}\right)_{Fr} d(PIF) + \left(\frac{\partial P}{\partial Fr}\right)_{PIF} d(Fr) \tag{3}$$

And the total penetration variation can be obtained by:

$$\int dP = \int \left(\frac{\partial P}{\partial PIF}\right)_{Fr} d(PIF) + \int \left(\frac{\partial P}{\partial Fr}\right)_{PIF} d(Fr) \tag{4}$$

or

$$\Delta P_{tot} = \Delta P_{PIF} + \Delta P_{Fr} \tag{5}$$

The term ΔP_{total} is the total penetration variation, and ΔP_{PIF} and ΔP_{Fr} are the individual penetration variations caused by changes in the PIF and Fr, respectively. Figure 3-11 illustrates Eq. 5 graphically. It shows that the total penetration variations can be estimated by adding the impact of individual PIF and frequency. This is obtained from the difference in penetrations measured between points D and A (where both Fr and PIF have changed, as occurred in a real respiration path). The individual effect of PIF can be estimated by the difference in penetrations between points A and C, or B and D. Similarly, the individual effect of Fr can be measured by the difference in penetrations between points A and B or C and D.

The ratio of individual penetration variations for each varying component to the total penetration variation is defined as the enhancement fraction value:

$$X_{PIF}(\%) = \frac{\Delta P_{PIF}}{\Delta P_{tot}} * 100\% \quad (6)$$

$$X_{Fr}(\%) = \frac{\Delta P_{Fr}}{\Delta P_{tot}} * 100\% \quad (7)$$

X_{PIF} and X_{Fr} represent the portions of penetration enhancement due to the PIF and breathing frequency, respectively.

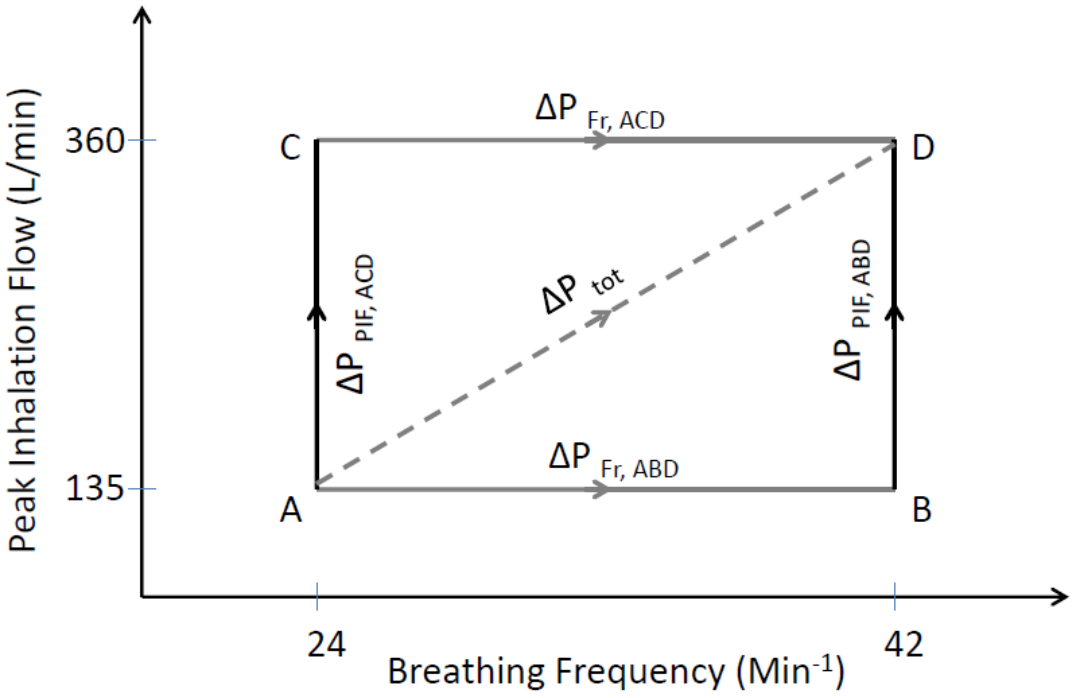

Figure 3-11: Penetration variations in terms of frequency or PIF

3.6.2 Experimental Conditions

Figure 3-12 shows four different cyclic flows (with sinusoidal pattern) used for this objective, consisting of two breathing frequencies (24 and 42 breaths per minute (BPM))

and two PIFs (135 L/min and 360 L/min). The summary of information regarding the cyclic flows selected is given in table 3-1 (flows A, B, C and D). For this objective, the tests were performed with both cyclic flow setups (figure 3-1a and b): "inhalation-and-exhalation" and "inhalation-only" setup.

The values of 135 and 360 L/min as PIF were selected to make an appropriate relevance to the real-world situation during workplace respiration with moderate to heavy workloads, respectively. For instance, 135 L/min as PIF (equal to 42 L/min as minute volume) is a good approximation to the moderate ventilation (minute volume) of 38.5 and 47.4 L/min as mean values suggested by Caretti et al. (2004) and Anderson et al. (2006), respectively. The selection of the first study was based on reviewing the data from physiological studies on human subjects during workplace breathing for occupational tasks. The second study was also performed on human subjects exercising under various workloads. Based on the appropriate relevance of cyclic flow with 135 L/min as PIF to the workplace breathing conditions, it has been frequently selected by several studies for filter performance evaluations (Richardson et al., 2006, Haruta et al., 2008, Cho et al., 2009, He et al., 2013a,b). The breathing frequency of 24 BPM selected by this study is also within the reported range of breathing rate suggested by Anderson et al. (2006) (26.5 ± 6.7 BPM). Although the occurrence of 360 L/min is not as frequent as 135 L/min, it has been reported by physiological literature during heavy workload respiration. This value (equal to 114 L/min as minute volume) corresponds to the average of the maximum flow rate measured at the end of exercise with a maximum workload performed on different human subjects (Blackie et al., 1991). The corresponding breathing frequency of 42 BPM was observed with this breathing flow. Almost a similar number (363.9 L/min as PIF)

was obtained by Berndtsson (2004) utilizing full-face masks for healthy human subjects when breathing in case of heavy workload. The same as 135 L/min, the value of 360 L/min has been also used for filter performance evaluation by other relevant studies (Eshbaugh et al., 2009; Mostofi et al., 2011). In overall, the selected PIFs and breathing frequencies used by this study cover breathings from a moderate to heavy workloads. The negative values of instant flow (exhalation cycle) in figure 3-12 are assumed to be zero for setup 2, since exhalation was eliminated from the cyclic flow. Temperature and relative humidity (RH) of the chamber, in this task, were 25 $\pm$ 3°C and 15 $\pm$ 5%, respectively.

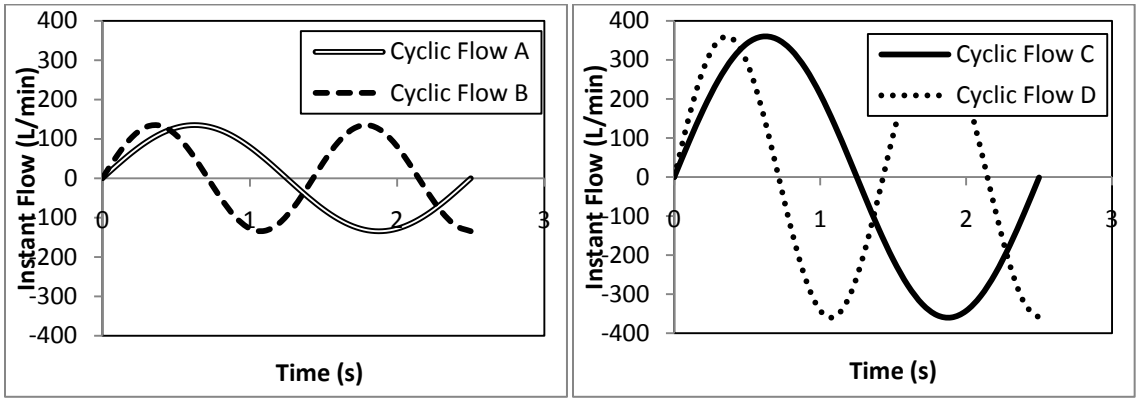

Figure 3-12: Selected cyclic flows for test criteria, objective 1

Table 3-1: Summary of cyclic flow information, objective 1

Cyclic Flows	Breathing Frequency (BPM)	Peak Inhalation Flow, PIF (L/min)	Tidal Volume (L)
(A)	24	135	1.771
(B)	42	135	1.013
(C)	24	360	4.792
(D)	42	360	2.741

3.6.3 Data Analysis

Each penetration measurement (poly-dispersed; 10-205.4 nm), for the four cyclic flows (see table 3-1), was repeated four times (N=4), and illustrated by the mean value and the standard deviation. Each experiment was repeated for the "inhalation-and-exhalation" and the "inhalation-only" setups (see figure 3-1a,b). The selection of flows A and D (see table 3-1) reflects the fact that, in practice, breathing frequency and PIF simultaneously increase. In order to consider the individual effects of frequency and inhalation flow, only one parameter is varied at a time, while the other was kept constant. Flows B and C were then added (see table 3-1). Consequently, according to figure 3-11, the two following paths could be assumed to separately address the impact of frequency and PIF:

1. Path ABD: First, increasing breathing frequencies only (from 24 to 42 BPM, while PIF is kept at 135 L/min), and then increasing PIF only (from 135 to

360 L/min while breathing frequency is kept at 42 BPM). The corresponding penetration differences are referred as $\Delta P_{Fr,ABD}$ and $\Delta P_{PIF,ABD}$, respectively.

2. Path ACD: First, increasing PIF only (from 135 to 360 L/min while breathing frequency is kept at 24 BPM), and then increasing breathing frequency (from 24 to 42 BPM while PIF is kept at 360 L/min). Corresponding penetration differences are cited as $\Delta P_{PIF, ACD}$ and $\Delta P_{Fr, ACD}$, respectively.

With the penetrations recorded, the most penetrating particle size (MPPS) range was obtained for each cyclic flow. Enhancement fraction values (X_{PIF} and X_{Fr}) were then calculated (by dividing ΔP_{PIF} and ΔP_{Fr} by the total penetration variation (ΔP_{tot})) for the MPPS range based on the two paths introduced above (see figure 3-11).

Using NCSS program software (NCSS, LLC Inc., Kaysville, UT, USA) the multiple comparison tests were applied by the analysis of variance (ANOVA) to check the significance of the potential affecting parameters: the breathing frequency, PIF, the experimental setup and their interactions on variations in penetration in the MPPS range. The values obtained for the penetration in the MPPS range were transformed to their logarithmic values as the response variable in the ANOVA. For each experimental setup, a separate two-way ANOVA for PIF and breathing frequency was performed. Finally a three-way ANOVA combining the data between setups 1 and 2 was applied to add the impact of experimental setup. Using descriptive statistics for each analysis, the normality of transformed penetrations was accepted by the Martinez-Iglewicz normality test.

3.7 Procedure for Objective 2

3.7.1 Experimental Conditions

Four cyclic flows with the peak inhalation flows of 135, 210, 270 and 360 L/min (indicated by group G3 to G6 in table 3-2) were primarily chosen. The corresponding breathing frequencies for these flows were 24, 30, 36 and 42 breaths per minute (BPM). For this objective, the tests for cyclic flows were performed with "inhalation-only" setup.

The principal for selection of the cyclic flows, having 135 and 360 L/min was previously explained in section 3.6.2. The cyclic flow with 270 L/min as PIF was selected to introduce cyclic flows with 85 L/min (certified by NIOSH) as minute volume, respectively. The cyclic flow with 210 L/min as PIF may simulate the mean breathing flow reported by Anderson et al. (2006) under heavy workload (mean PIF of 218.4 ± 53.7 L/min with corresponding breathing frequency of 31.9 ± 7.4 BPM).

The penetrations obtained for each of the above-mentioned cyclic flows was accompanied by the measurement of penetrations achieved under three constant flows equivalent to minute volume, MIF and PIF of the same cyclic flow (flows indicated in the same row in table 3-2). To have a large set of data for comparison, another four cyclic flows possessing equivalent MIFs of 42, 68, 270 and 360 L/min were selected (see table 3-2). They were presented in groups G1, G2, G7 and G8, respectively. The corresponding PIF for these flows were 68, 105, 430 and 570 L/min. The first two flows (68 and 105 L/min as PIF) normally reflect the breathing achieved by sedentary to moderate workload breathing. Despite the selection of the last two cyclic flow rates was too conservative, the cyclic flow with 430 L/min as the PIF can be estimated as the upper standard

deviation of the breathing during the highest workload (363.9 ± 66.3 L/min) reported by Berndtsson (2004). Similar value has been also reported by Blackie et al. (1990). The cyclic flow with 570 L/min may also represent the upper 95 % percentile of high workload breathing when the subjects made speech during exercise (reported as 573 L/min by Berndtsson (2004)). The relative humidity (RH) and the temperature of the chamber were kept at 15 ± 5 % and 25 ± 3 °C, respectively.

Table 3-2: Constant and cyclic flow selections; objective 2

Flow groups	Cyclic Flows (Fr (BPM); PIF (L/min))	Constant flow (equal to cyclic minute volume), L/min	Constant flow (equal to cyclic MIF), L/min	Constant flow (equal to cyclic PIF), L/min
G1	Fr=16, PIF=68	N/A	42	68
G2	Fr=20, PIF=105	N/A	68	N/A
G3	Fr=24, PIF=135	42	85	135
G4	Fr=30, PIF=210	68	135	210
G5	Fr=36, PIF=270	85	170	270
G6	Fr=42, PIF=360	115	230	360
G7	Fr=45, PIF=430	135	270	N/A
G8	Fr=48, PIF=570	N/A	360	N/A

3.7.2 Data Analysis

The penetration measurements were carried out for both cyclic and constant flows and repeated five times for each flow, and the values were illustrated by their mean value and

standard deviations (N=5). Subsequently, for each flow, the MPPS was obtained. For comparison of the penetrations achieved by the cyclic flow and the constant flows equivalent to cyclic MIF, the statistical analysis was performed by one-way and two-way analysis of variance (ANOVA). First, the binary comparisons for maximum penetrations (response variable) were executed by one-way ANOVA (pattern of flow: cyclic or constant, was determined as the factor variable). Second, a two-way ANOVA was carried out to investigate the impact of factor variables: flow magnitude, flow pattern (cyclic or constant) and their interactions on the maximum penetration (response). For the two-way ANOVA the data corresponding to constant and cyclic flows rates (with the same MIF) of 42 and 68 L/min were not considered by the analysis to keep the pooled data proximate to the normal distribution by descriptive statistics, since a significant deviation from normal distribution took place when the penetration data for these flow rates was included, in the analysis.

3.8 Procedure for Objective 3

3.8.1 Experimental Conditions

Two constant flows with the magnitudes of 85 and 170 L/min and a cyclic flow with the peak inhalation flow (PIF) of 270 L/min (minute volume of 85 L/min) were selected for the experiments of this study. The same as objective 2, the tests for cyclic flows are performed with “inhalation-only” setup.

Penetrations were obtained at the initial time (zero) and 2 hours, 4 hours and 6 hours from the initial time of the test. To make sure that the upstream concentration was in an appropriate stable condition during the 6-hour test, the four recorded upstream

concentration distributions (measured at initial time, 2-hour, 4-hour and 6-hour) were compared with each other and the deviation among the four samples were evaluated. The maximum and the average deviation among samples did not exceed 17 % and 8 %, respectively; suggesting that the upstream concentration has been in an appropriate state of stability during the whole test time. The relative humidity and the temperature of the chamber, for the flow rates selected in this objective was kept at 10 % and 25 ± 3 ºC, respectively.

3.8.2 Data Analysis

For each selected flow rate, five respirators were tested (N=5), each for a period of 6-hour loading time. The penetration values for each of the flow rates and loading times were then illustrated with the mean values and standard deviation. The comparison tests were performed with one-way and two-way ANOVA to verify the significance of factor variables and interactions on the maximum penetration at MPPS. The effect of the loading time (at initial, 2nd hour, 4th hour and 6th hour) was verified by the one-way ANOVA for each of the selected flows. The simultaneous impact of flow pattern (constant or cyclic) and loading time was also considered using two-way ANOVA (the constant flow in the latter analysis was considered as MIF). Only for the one-way ANOVA corresponding to the loading time effect on the constant flow rate of 85 L/min, a log-transformation was accomplished to normalize the pooled data. For other analysis performances, however, no transformation was done, since the normality of the pooled data was already accepted by the descriptive statistics.

CHAPTER 4: RESULTS AND DISCUSSIONS

4.1 Contribution of Breathing Frequency and Peak Inhalation Flow on Performance of N95 Filtering Facepiece Respirators

4.1.1 Results for "Inhalation and Exhalation" Setup (Setup 1)

4.1.1.1 Penetration vs. PIF and Breathing Frequency

Figure 4-1 indicates challenge concentration distributions in terms of particle size at the N95 FFR upstream for the four cyclic flows A, B, C and D. The summary of statistical information for each concentration curve is given in table 4-1.

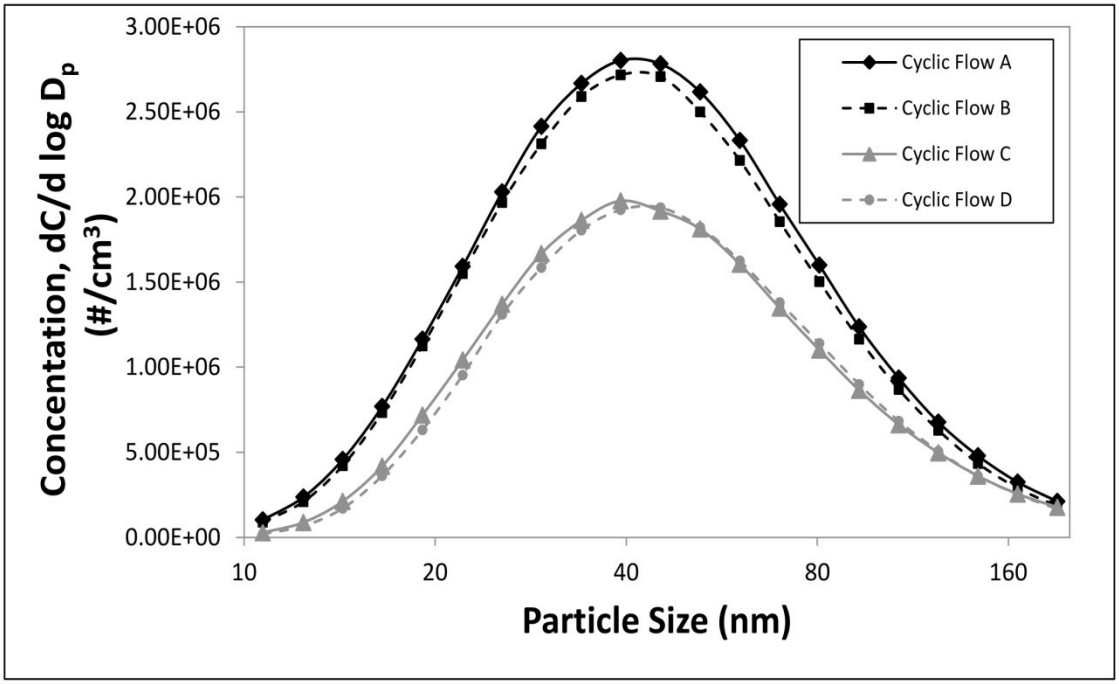

Figure 4-1: Typical concentration distribution of N95 FFR upstream for the four tested flows for setup 1

Table 4-1: NaCl challenge concentration distribution characteristics for setup 1

Cyclic Flow	Count Median Diameter (nm)	Geometric Standard Deviation	Peak Concentration (#/cm^3) @ Peak Size (nm)	Total Concentration (#/cm^3) (Normalized by log D_p)
A (PIF=135, Fr= 24)	43.3	1.79	2.80E6 (@39.2 nm)	1.84E6
B (PIF=135, Fr= 42)	43.1	1.77	2.72E6 (@39.2 nm)	1.76E6
C (PIF=360, Fr= 24)	44.3	1.77	1.98E6 (@39.2 nm)	1.25E6
D (PIF=360, Fr= 42)	45.6	1.75	1.94E6 (@45.3 nm)	1.23E6

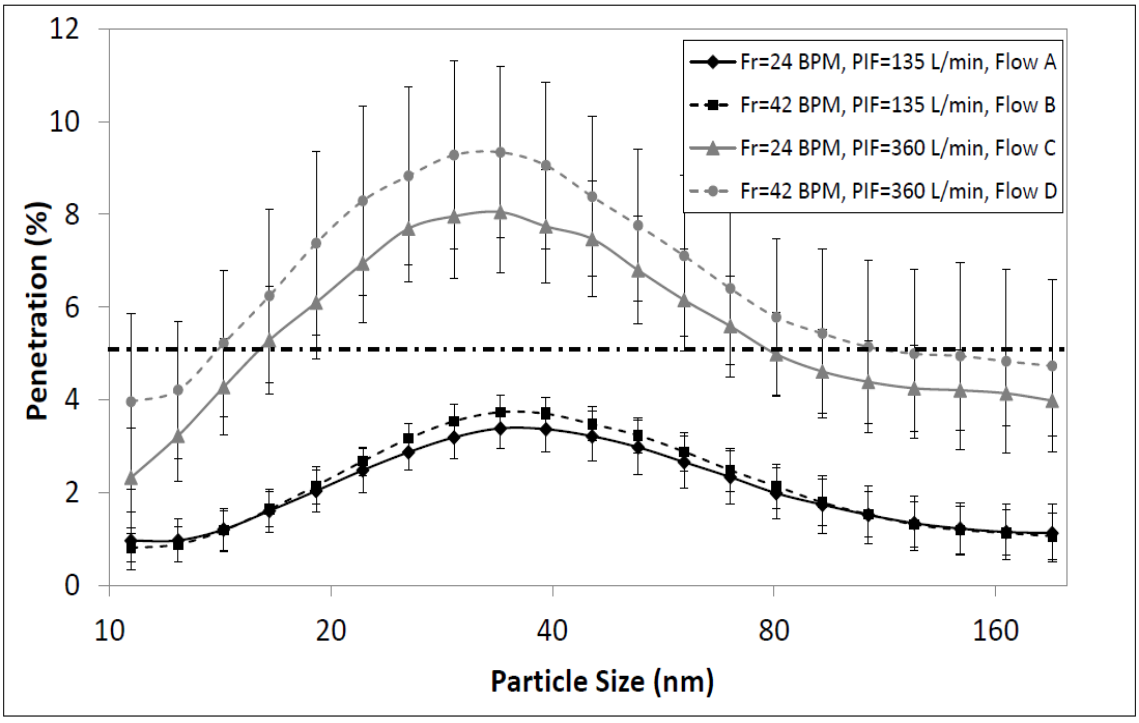

Figure 4-2: Penetration of NaCl particles through N95 FFR for the tested cyclic flows for setup 1

Figure 4-2 demonstrates the penetration of 10–205.4 nm NaCl particles through the tested N95 FFRs for all the cyclic flows. The maximum values for the penetrations normally occurred within the range of 29.4–39.3 nm (MPPS range). As illustrated, compared with flow A (lowest frequency and PIF), the penetrations under flows B, C and D were increased. This indicated that both frequency and PIF were influential in enhancing the magnitude of penetration; nonetheless, the impact of PIF was observed to be much more pronounced than the frequency. For path ABD (see figure 3-11) for instance, the average penetration at MPPS range reached 3.31, 3.66 and 9.22% for the three cyclic inhalation flows A, B and D, respectively. This corresponds to only an 11% increase in penetration when the frequency was changed from 24 to 42 BPM (point A to point B). A 152% increase in penetration also occurred when the PIF was varied from 135 to 360 L/min (point B to point D). Similarly for path ACD (where penetration of the MPPS range under flow C reached 7.92%), a 139% increase in penetration was observed when the PIF was changed from 135 to 360 L/min (point A to point C), and only 16% when the frequency was varied from 24 to 42 BPM (point C to point D). These percentages suggest that the impact of breathing frequency on penetration increase is almost negligible compared with the PIF. Statistical analysis, achieved by two-way ANOVA, illustrated the significant impact on penetrations as a result of PIF ($p<0.001$), and insignificant impact due to Fr ($p=0.123$). The analysis suggested no significant interaction between two parameters ($p=0.764$).

4.1.1.2 Enhancement Fraction Values

The enhancement fraction values (X_{PIF} and X_{Fr}) can help in interpreting the relative contribution of PIF and breathing frequency as the characteristic properties of breathing

flow. For path ABD (see figure 3-11), the frequency enhancement fraction value did not exceed 6% and the rest of the enhancement (94%) was due to PIF variations. The same qualitative results (higher PIF fractions) were also recorded for path ACD where 22% and 78% were respectively calculated as frequency and PIF enhancement fractions. The higher enhancement fraction value for frequency for path ACD indicates that the penetration's sensitivity to the variations in frequency for high PIFs is greater than for low PIFs. In other words, as the PIFs increase, breathing frequency becomes more important, even though its overall role is still not as significant as the PIF impact. The latter fact is, however, based on the results obtained from experimental data. Further theoretical research is needed to investigate this phenomenon.

4.1.2 Results for "Inhalation Only" Setup (Setup 2)

4.1.2.1 Penetration vs. PIF and Breathing Frequency

The same approach used for the "inhalation-and-exhalation" scenario was applied to the case of "inhalation-only" (setup 2). The summary of challenge concentration distributions and statistical information is available in figure 4-3 and table 4-2.

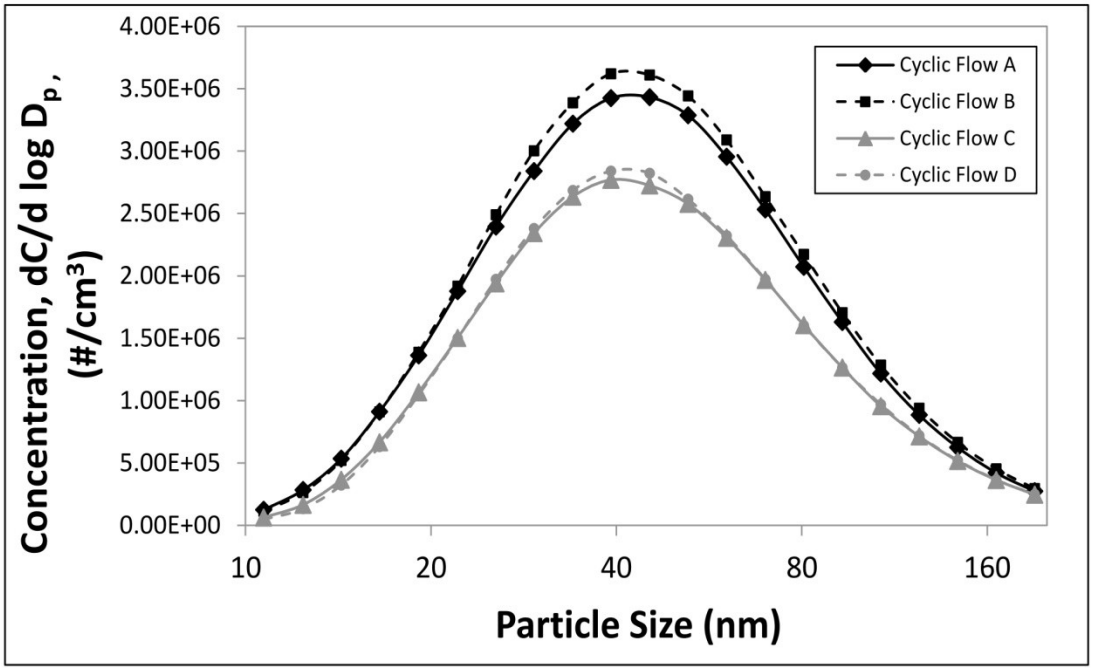

Figure 4-3: Typical concentration distribution of N95 FFR upstream for the four tested flows for setup 2

Table 4-2: NaCl challenge concentration distribution characteristics for setup 2

Cyclic Flow	Count Median Diameter (nm)	Geometric Standard Deviation	Peak Concentration (#/cm^3) @ Peak Size (nm)	Total Concentration (#/cm^3) (Normalized by log D_p)
A (PIF=135, Fr= 24)	44.5	1.79	3.43E6 (45.3 nm)	2.27E6
B (PIF=135, Fr= 42)	44.7	1.78	3.62E6 (39.2 nm)	2.37E6
C (PIF=360, Fr= 24)	44.4	1.78	2.77E6 (39.2 nm)	1.80 E6
D (PIF=360, Fr= 42)	44.5	1.77	2.84 E6 (39.2 nm)	1.81 E6

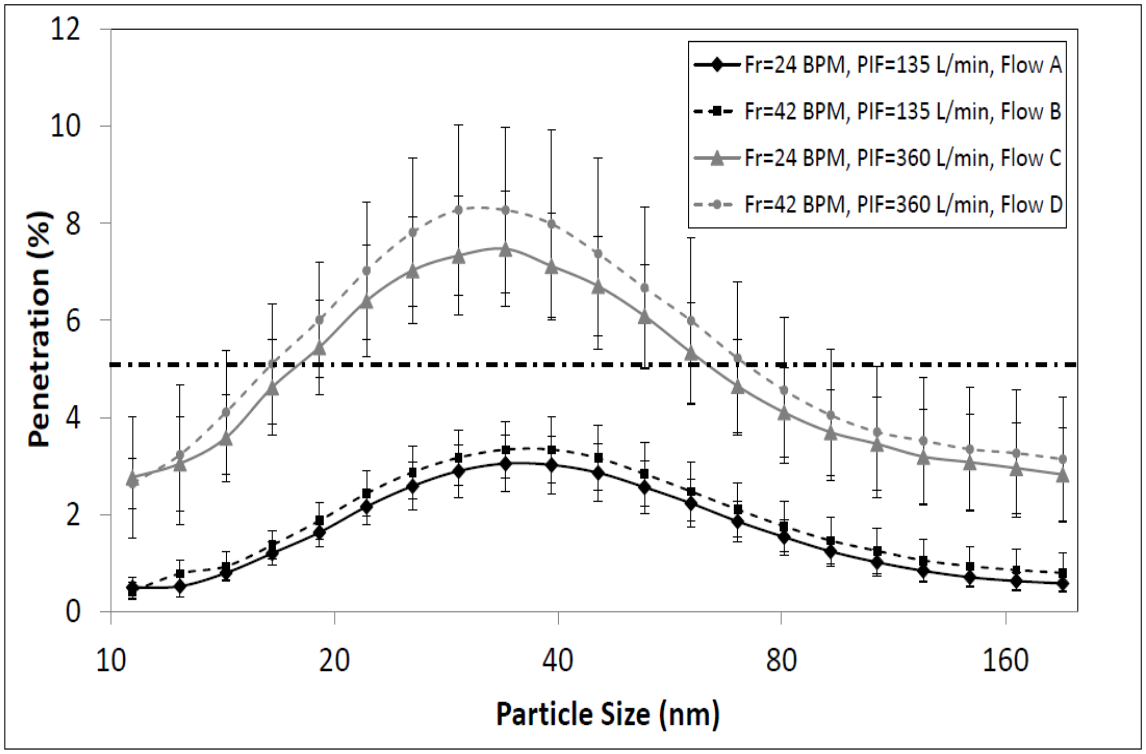

Figure 4-4: Penetration of NaCl particles through N95 FFR for the tested cyclic flows for setup 2

Figure 4-4 illustrates the penetrations measured within the entire tested range (10–205.4 nm) for the four selected cyclic flows for "inhalation-only" setup. Penetration normally reached its highest values within the range of 29.4–39.3 nm (MPPS). As demonstrated, in the MPPS range, the measured penetrations were 2.99, 3.28, 7.31 and 8.02% for the four tested flows, respectively. This suggests that a 10% increase in the penetration was observed when the frequency increased from 24 to 42 BPM (path ABD in figure 3-11, from flow A to flow B). On the other hand, a 145% increase was observed by increasing the PIF from 135 to 360 L/min (from flow B to flow D). Similarly, a 144% increase in penetration was observed when the PIF was increased from 135 to 360 L/min (path ACD, from flow A to flow C). It is also shown that only a 10% increase was observed when the frequency was varied from 24 to 42 BPM (from flow C to flow D). Using two-way

ANOVA, a statistically significant change in penetration could be seen by PIF variations ($p<0.001$), while the change caused by frequency was not as significant as that caused by PIF ($p=0.332$). Similar to experimental setup 1 (inhalation and exhalation setup), no effective interaction was detected between two parameters ($p=0.987$).

4.1.2.2 Enhancement Fraction Values

Similar methodology, used in setup 1 (both inhalation and exhalation), for calculation of enhancement fraction values (X_{PIF} and X_{Fr}), was applied to experimental setup 2 (inhalation only) to investigate the contribution of PIF and frequency. For instance, for path ABD (see figure 3-11), the frequency and PIF enhancement fractions are 6 and 94%, respectively. Similarly, 14 and 86% were respectively calculated as frequency and PIF enhancement fractions for path ACD.

The indicator dashed line in figures 4-2 and 4-4 shows the NIOSH 5% allowable limit for N95 FFRs (42 CFR, 84). It should, however be noted that the current test protocol is different from NIOSH certification. First, NIOSH uses a constant flow with rate of 85 L/min rather than a cyclic flow. Second, NIOSH measures the penetration at a mass median diameter (MMD) of 300 nm particle based on the light scattering method to record the concentration upstream and downstream. In this study, poly-dispersed particles were used with the SMPS as the measurement technique. As seen in figure 4-2 for setup 1, penetration of particles were reported above 5% within the 16.5–80.6 nm range for case C (PIF=360, Fr= 24) and 14.3–107.5 nm for case D (PIF=360, Fr= 42). This shows that under high PIFs (360 L/min), the range of UFPs penetration exceeds the NIOSH threshold limit. The enhancement of penetration by increasing the PIF is attributed to the

fact that with higher inhalation flows, the rate of major capturing mechanisms (electrostatic and diffusion) is considerably reduced. This is consistent with the result of Richardson et al. (2006), Haruta et al. (2008), Eshbaugh et al. (2009) and Wang et al. (2012) for cyclic flows at higher PIF values. On the other hand, penetration does not exceed the 5% limit at 135 L/min PIF for all frequencies. To better verify the impact of frequency, more tests were carried out with a complementary cyclic flow for setup 1 with an extremely high frequency of 85 BPM and PIF of 135 L/min. Similar to the other flows, the penetration within the entire tested range (10–205.4 nm) was then measured and the penetrations in the MPPS range (representing the worst-case scenario) were reported and compared with cases A and B with 135 L/min as PIF (see figure 4-5). This figure shows that the MPPS penetration for all frequencies having the same PIF (135 L/min) is always under the threshold limit of 5%. Unlike PIF, an increase in frequency can rarely vary the filtration mechanisms, since the penetration variations do not take place in the same way as what occurs for the PIF. The low variation in penetration by frequency (in nano-metric range) is consistent with the result of Wang et al. (2012) (tested for 0.3 μm size). As confirmed in this study, the MPPS was recorded for all selected flows for sizes below 100 nm, which confirms the presence of electrostatic attraction mechanism in N95 FFRs (Martin and Moyer, 2000; Balazy et al., 2006a; Richardson et al., 2006; Eninger et al., 2008; Mostofi et al., 2011).

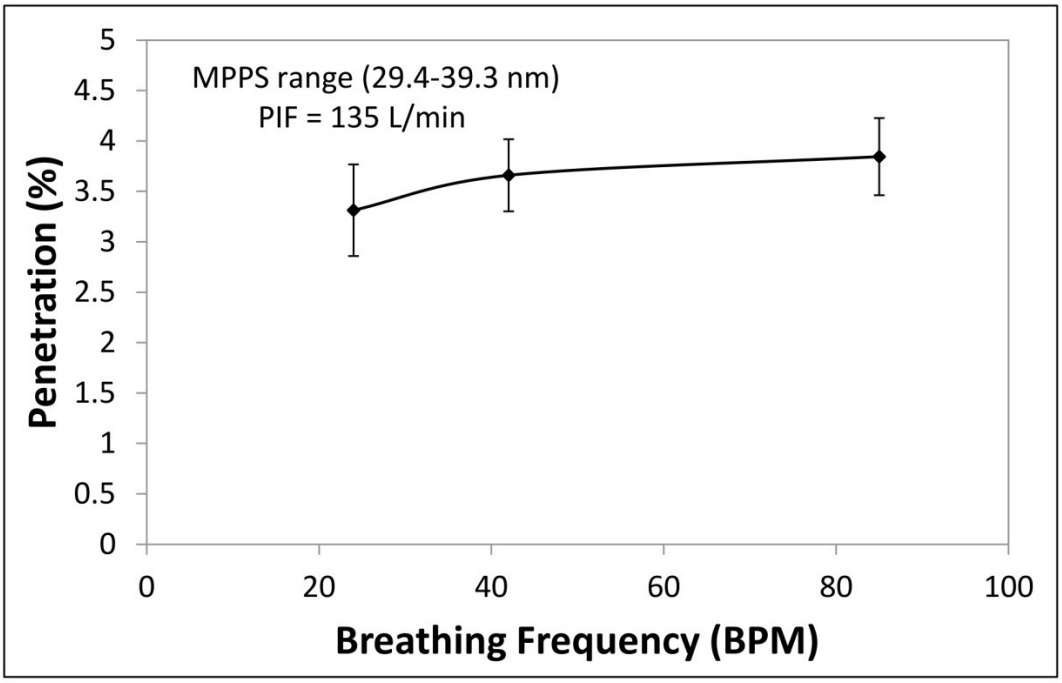

Figure 4-5: Penetration at MPPS range for cyclic flows with 135 L/min as PIF versus frequency (24, 42 and 85 BPM) for N95 FFR - Experimental setup 1.

4.1.3 Impact of Experimental Setup

As stated earlier, two different experimental setups were used in this study: the first setup included both inhalations and exhalations through the filter media, while the second setup included only inhalation. Even though we observed almost similar results from the two experimental setups, we did notice a difference in the penetration: the penetration values for setup 1 were slightly higher than the values for cases in setup 2. However, it should be noted that the statistical analysis indicates that such an increase is not significant. The three-way ANOVA for the results of setups 1 and 2 for the PIF, frequency and experimental setups shows -a substantial impact by PIF ($p<0.001$), but not a significant impact of frequency and experimental setup ($p>0.05$). No effective interaction was also detected between any of these factors ($p>0.05$). The slight increase in penetration for

setup 1 (inhalation and exhalation) could be attributed to the fact that the exhaled air may remove some of the particles on the surface of the N95 and make it easier for diffusion and penetration of upstream particles in the next inhalation cycle. Figure 4-6 summarizes the measured penetration for the MPPS range for all tested cyclic flows for setups 1 and 2.

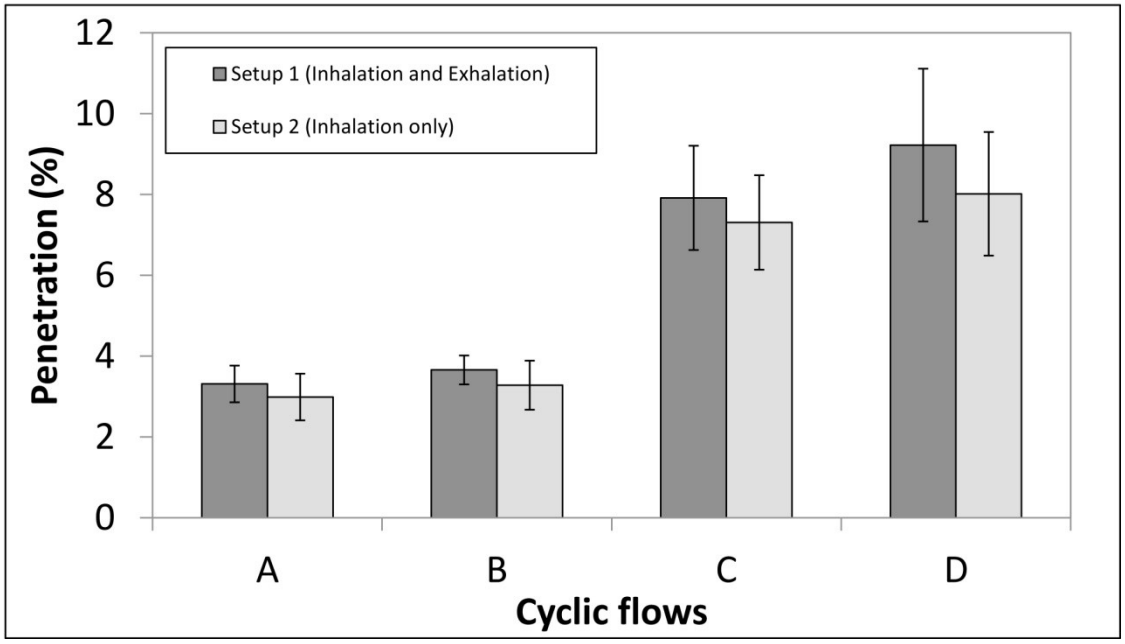

Figure 4-6: Comparison of penetrations at MPPS range for cyclic flows A, B, C and D between for 1 and 2

4.2 Investigation of N95 Filtering Facepiece Respirator Efficiency against Ultrafine Particles Performed with Cyclic and Constant Flows

4.2.1 Concentration Distributions

The challenge concentration provided in this objective for all constant and cyclic flows was poly-dispersed generated by a 6-jet Collison nebulizer (0.1 v/v NaCl solution). Figure 4-7 illustrates the typical upstream concentration distribution within the range of 10-205.4 nm for cyclic flow with equivalent 270 L/min as PIF (or minute volume of 85 L/min).

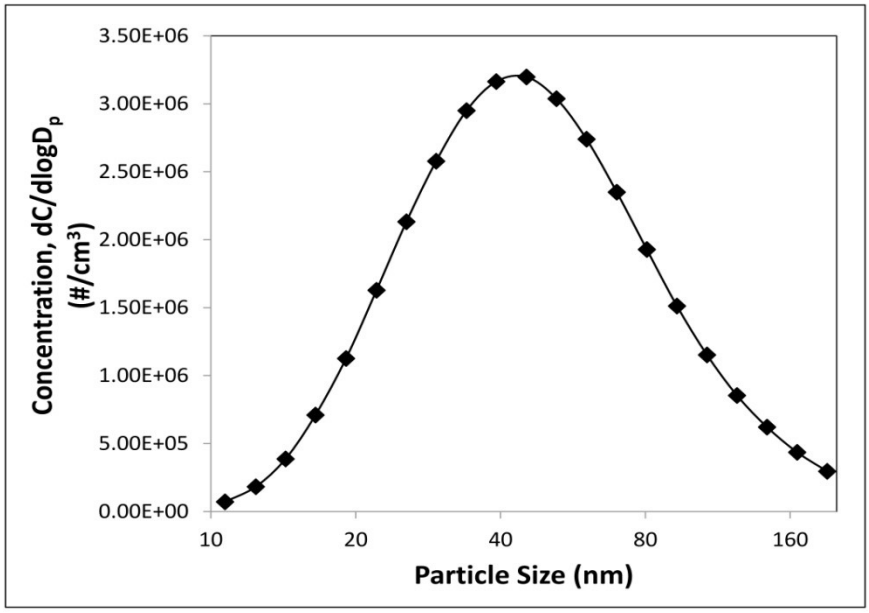

Figure 4-7: Typical concentration distribution of N95 FFR upstream for cyclic flow with 270 L/min as PIF

4.2.2 Penetration in Terms of Constant and Cyclic Flow

The penetration curves (in terms of particle size) for cyclic flows with equivalent PIFs of 135, 210, 270 and 360 L/min (groups of G3, G4, G5 and G6 in table 3-2) for 10-205.4 nm particles are illustrated in figures 4-8 to 4-11, respectively (solid black lines). Each cyclic

flow curve is accompanied by three other curves corresponding to the penetration under constant flows equivalent to cyclic flow minute volume, MIF and PIF (indicated by dashed grey lines).

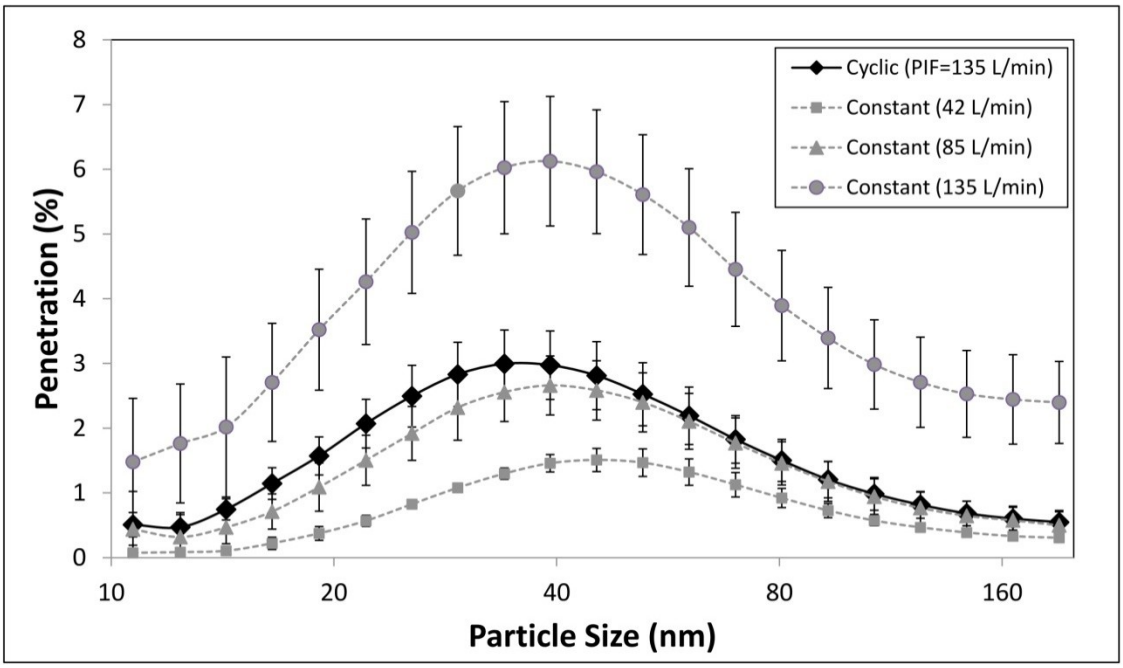

Figure 4-8: Penetration of NaCl particles: cyclic flow (135 L/min as PIF, 85 L/min as MIF and 42 L/min as minute volume); constant flows (42, 85 and 135 L/min)

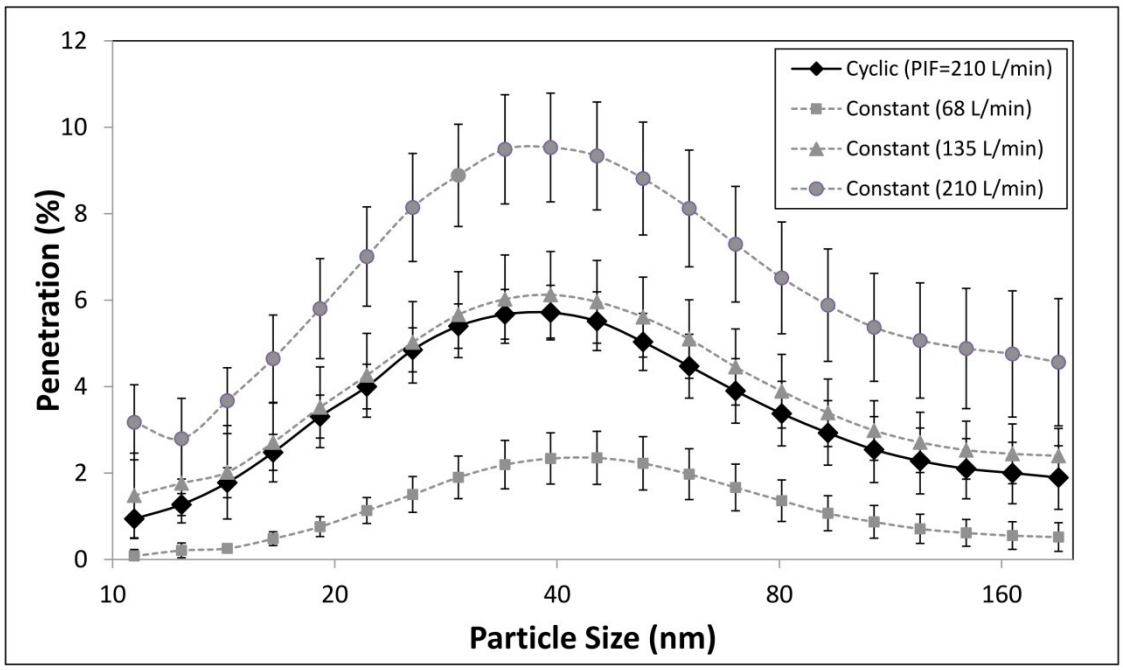

Figure 4-9: Penetration of NaCl particles: cyclic flow (210 L/min as PIF, 135 L/min as MIF and 68 L/min as minute volume); constant flows (68, 135 and 210 L/min)

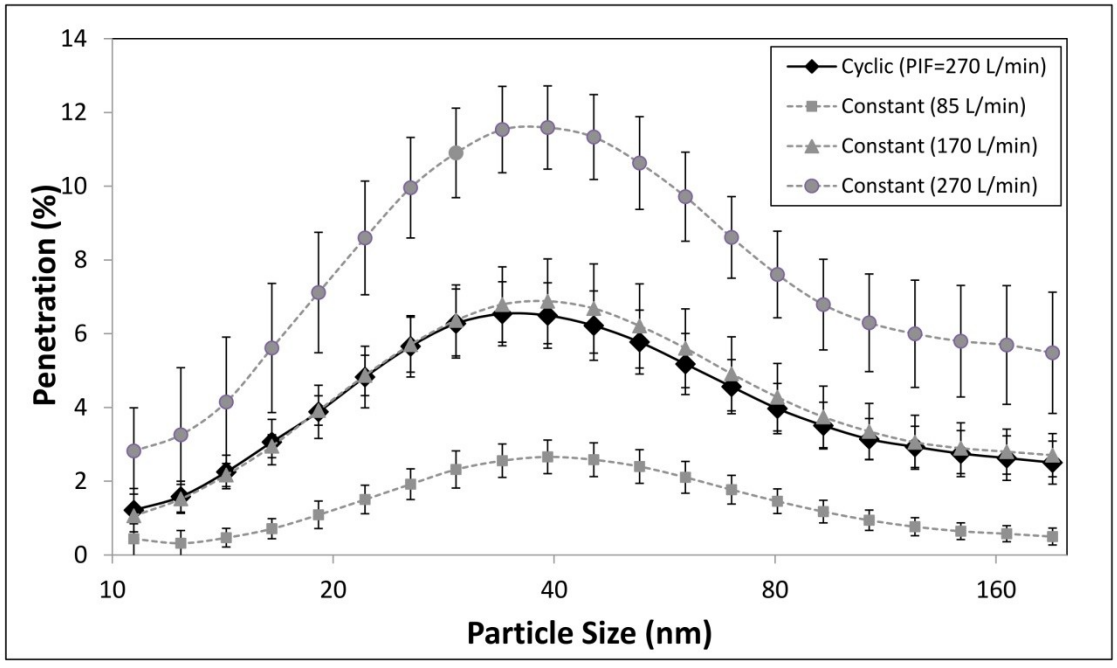

Figure 4-10: Penetration of NaCl particles: cyclic flow (270 L/min as PIF, 170 L/min as MIF and 85 L/min as minute volume); constant flows (85, 170 and 270 L/min)

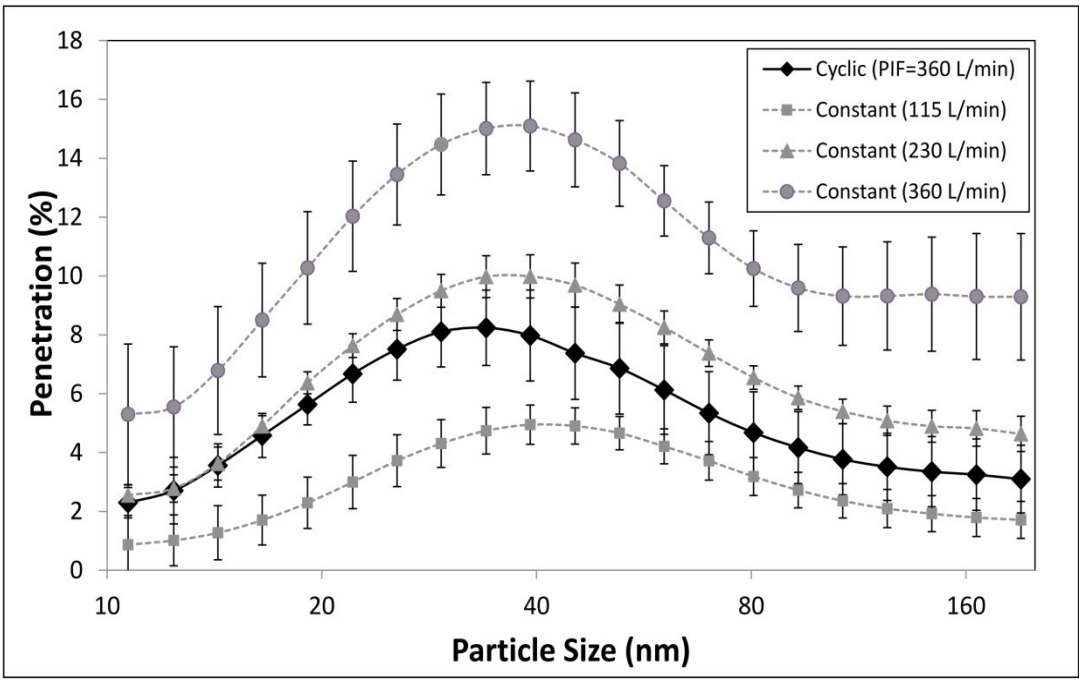

Figure 4-11: Penetration of NaCl particles: cyclic flow (360 L/min as PIF, 230 L/min as MIF and 115 L/min as minute volume); constant flows (115, 230 and 360 L/min)

As indicated in figures 4-8 to 4-11 (penetration in terms of particle size), regardless of the magnitude of selected cyclic or constant flows, the penetration measured under cyclic flow was always higher than the penetration measured under the constant flow equivalent to the minute volume of the cyclic flow. For example the maximum penetration under the constant flow rate of 85 L/min reached 2.66 ± 0.46%, while for the cyclic flow having the same flow rate as minute volume (270 L/min as PIF) it reached 6.54 ± 0.87%. This shows that the constant flow equal to the cyclic flow minute volume underestimates the cyclic flow in terms of penetration. On the other hand, since NIOSH selection is the 85 L/min constant flow as the minute volume of the breathing under high workloads, it is necessary to verify the penetration by cyclic flow as well, due to the significant increase in penetration occurred by the cyclic flow compared to the constant flow (minute volume). The lower penetration under constant flow (minute volume) compared to the cyclic flow

is consistent with the earlier results (Stafford et al., 1973, Brosseau et al., 1990, Eshbaugh et al., 2009 and Wang et al., 2012). The similarities among all these findings (despite variations in the experimental setups and conditions) suggest that the lower penetration recorded for the constant flow (minute volume), is independent of the setup and conditions (such as magnitude of flow, filter type, particle material, size and distributions).

Compared to the minute volume, an inverse situation takes place when the penetration by the cyclic flow is compared with a constant flow equivalent to the cyclic PIF. For example, the penetration under cyclic flow with 270 L/min as the equivalent PIF and the constant flow having the same flow rate were recorded as 6.54 ± 0.87 and 11.59 ± 1.13 %, respectively. This reveals that the selection of constant flow equal to the PIF overestimates the penetration obtained by the cyclic flow. The latter is consistent with the result of Richardson et al. (2006), Eshbaugh et al. (2009) and Wang et al. (2012), despite the difference in selection of filter types, particle materials and size ranges.

Unlike the minute volume and PIF, the constant flow equivalent to the cyclic flow MIF typically gives better estimation of the penetration values when compared to the cyclic flow. For example, the maximum penetrations measured under the cyclic flow with 170 L/min flow rate as MIF (PIF of 270 L/min) and constant flow (same magnitude) were recorded as 6.54 ± 0.87 and 6.88 ± 1.15, respectively. This cyclic flow (170 L/min flow rate as MIF) indicates the flow rate which corresponds to the NIOSH certification (since the minute volume for this flow rate is 85 L/min). The percentages of penetration (in MPPS) for these flow rates demonstrates that instead of the constant flow equal to cyclic

flow minute volume, the constant flow equal to cyclic flow MIF (a doubled flow compared to minute volume) is a better estimator of the penetration under cyclic flow.

4.2.3 Maximum Penetration in Terms of Flow Magnitude and Pattern

Table 4-3 summaries the maximum penetrations (at MPPS) and the MPPS channels for flow groups of G1 to G8 (see table 3-2). Figure 4-12 presents the maximum penetrations for all the investigated flows (groups G1 to G8, see table 3-2). Maximum penetrations for the cyclic flows are illustrated by three different curves by its minute volume, by its MIF, and by its PIF. For both cyclic and constant flows, the maximum penetrations (at MPPS) were almost linearly increased with the enhancement of flow rates and tend to zero penetrations at very low flow rates.

Table 4-3: Summary of maximum penetration and MPPS information for various constant and cyclic flows

	Maximum Penetration (%)				MPPS (nm)			
Flow groups	Cyclic flow (equivalent PIF)	Constant flow (Min. Vol.)	Constant flow (MIF)	Constant flow (PIF)	Cyclic	Constant (Min. Vol.)	Constant (MIF)	Constant (PIF)
G1	1.55 ± 0.27 (68 L/min)	N/A	1.51 ± 0.18 (42 L/min)	2.35 ± 0.61 (68 L/min)	39.2	N/A	45.3	45.3
G2	2.53 ± 0.75 (105 L/min)	N/A	2.35 ± 0.61 (68 L/min)	N/A	39.2	N/A	45.3	N/A
G3 (figure 4-8)	2.99 ± 0.52 (135 L/min)	1.51 ± 0.18 (42 L/min)	2.66 ± 0.46 (85 L/min)	6.12 ± 1.00 (135 L/min)	34	45.3	39.2	39.2
G4 (figure 4-9)	5.71 ± 0.63 (210 L/min)	2.35 ± 0.61 (68 L/min)	6.12 ± 1.00 (135 L/min)	9.53 ± 1.26 (210 L/min)	39.2	45.3	39.2	39.2
G5 (figure 4-10)	6.54 ± 0.87 (270 L/min)	2.66 ± 0.46 (85 L/min)	6.88 ± 1.15 (170 L/min)	11.59 ± 1.13 (270 L/min)	34	39.2	39.2	39.2
G6 (figure 4-11)	8.24 ± 1.28 (360 L/min)	4.95 ± 0.67 (115 L/min)	9.99 ± 0.73 (230 L/min)	15.10 ± 1.53 (360 L/min)	34	39.2	39.2	39.2
G7	9.42 ± 1.62 (430 L/min)	6.12 ± 1.00 (135 L/min)	11.59 ± 1.13 (270 L/min)	N/A	34	39.2	39.2	N/A
G8	12.35± 1.14 (570 L/min)	N/A	15.10 ± 1.53 (360 L/min)	N/A	34	N/A	39.2	N/A

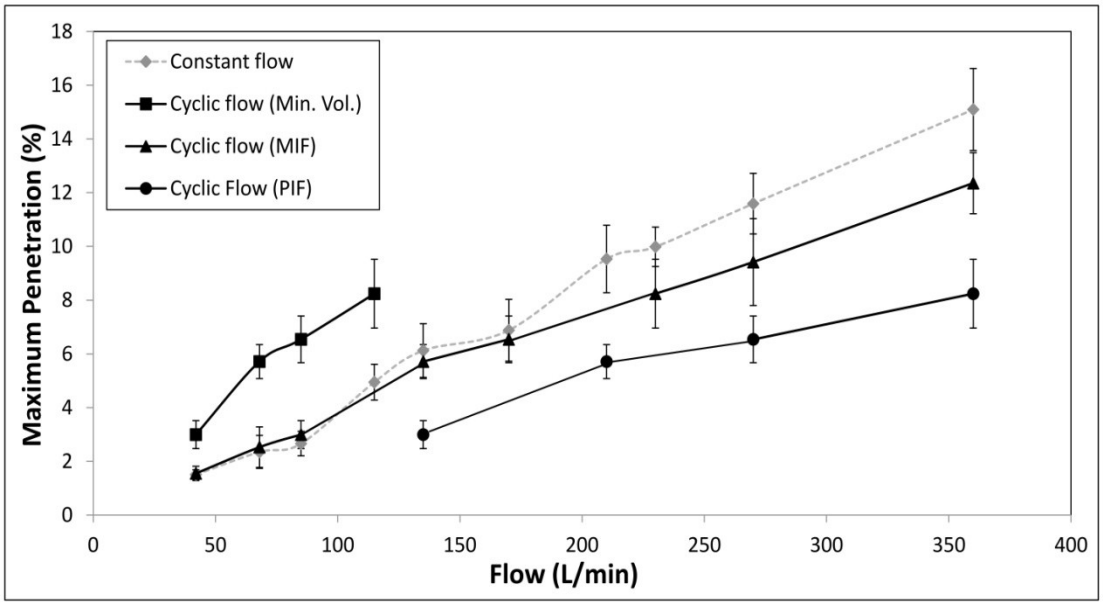

Figure 4-12: Maximum penetration in terms of constant and cyclic flows (with equivalent minute volume, MIF and PIF)

Figure 4-12 clearly demonstrates that the constant flow equivalent to the MIF can best represent the penetrations that can be obtained by a cyclic flow (with the same MIF) (the worst-case scenario penetration). For the first three flow comparisons (42, 68 and 85 L/min; groups of G1, G2 and G3 in table 3-2) a slight increase was observed by cyclic flows rather than the constant flows. For the next selected flows (groups G4 to G8 in table 3-2), however, the maximum penetrations under constant flow were higher than the maximum penetration observed under cyclic flow. The statistical analysis for binary comparisons between the constant and cyclic flows by one-way ANOVA indicated that the difference between the flows in groups G1 to G5 (42 to 170 L/min) was not significant ($p>0.05$). The comparison between the last three flows (G6, G7 and G8; 230 to 360 L/min) suggested that the difference between the maximum penetrations measured by the cyclic and constant flow was statistically significant ($p<0.05$). Table 4-4 gives the statistical analysis for the binary comparisons between the constant and cyclic flows.

Table 4-4: Summary of one-way ANOVA for maximum penetrations by constant and cyclic flow

Flow (Constant or cyclic with same MIF; L/min)	P-value	Flow (Constant or cyclic with same MIF; L/min)	P-value
42	0.775	170	0.612
68	0.697	230	0.029*
85	0.311	270	0.039*
135	0.450	360	0.012*

* Statistically significant ($p<0.05$), rejects null hypothesis

The results for the two-way ANOVA indicated a statistically significant difference as a result of both flow magnitude and flow pattern ($p<0.001$), and their interaction ($p<0.05$). The effective interaction between the variables: flow magnitude and flow pattern reveals that depending on the magnitude of flow rates for comparison of the penetration measured between constant and cyclic flows, equal or different penetrations could be achieved. This is consistent with the results of Haruta et al. (2008). Such interaction between two factor variables (flow magnitude and flow pattern) could be visible from the data shown in figure 4-12, since for the lowest flows almost same results were obtained for the maximum penetration. On the other hand, for higher flow rates, not equal maximum penetrations were observed. Table 4-5 gives the summary of the two-way ANOVA applied for comparison of constant and cyclic flows.

Table 4-5: Summary of two-way ANOVA for maximum penetrations in terms of flow pattern (constant and cyclic flow) and magnitude

Factor variables	P-values
Flow magnitude	0.000*
Flow pattern (constant or cyclic)	0.000*
Flow magnitude * flow pattern	0.014*

* Statistically significant ($p<0.05$), rejects null hypothesis

The findings of this study for the comparison of constant and cyclic flow impact on particle penetration are not always consistent with the results of Richardson et al. (2006), Eshbaugh et al. (2009) and Wang et al. (2012). The constant flow equivalent to MIF, in this study, is suggested to give equal or higher penetration compared with the cyclic flow. That is mainly due to variations of some of parameters such the type and model of test filter (one model of N95 FFRs) and type of particle (NaCl), the experimental set-up (use of manikin). However, the results of Eshbaugh et al. (2009) and Richardson et al. (2006) are generalized for various types of N95 and P100 (FFRs and cartridges) and various particle materials (NaCl, DoP, PSL and Emery 3004). Additionally the sub-micrometer challenge particles selection in Richardson et al. (2006) was based on mono-dispersed generations, while this study applied the poly-dispersed particles.

The findings of this study, on the other hand, showed more consistency with the results of Haruta et al. (2008), since there was tendency in penetration under constant flows to exceed the penetrations under the cyclic flow at increased flow rates. It should be regarded that both studies used a manikin-based protocol, while Richardson et al. (2006) and Eshbaugh et al. (2009) did not use manikin head to hold the filters. Further theoretical research work is required to have a better understanding of this process and the impact of influencing parameters of the filter performance. Of course, in spite of the similarity between the results of this study and Haruta et al. (2008), it was noted that the significance in the maximum penetration recorded between constant and cyclic flows could be obvious with very high flow rates (higher than the selected values in Haruta et al. (2008)). The difference could be attributed to the type of particle materials tested (NaCl versus PSL) and different particle type (poly-dispersed versus mono-dispersed).

The MPPS channels for various tested constant and cyclic flows were located at 34, 39.2 or 45.3 nm size channels (see table 4-3). These values confirmed the presence of electrostatic attraction in addition to the diffusion and interception mechanisms which significantly shifts the location of MPPS towards the sizes less than 100 nm compared to mechanical filters where MPPS takes places at almost 300 nm. The latter is consistent with several earlier studies carried out for N95 respirators (Martin and Moyer, 2000, Balazy et al., 2006a, Eninger et al., 2008, Eshbaugh et al., 2009, Mostofi et al., 2011). The results showed that the MPPS tended to slightly shift towards the larger sizes, when the flow rate was lowered. For example, among constant flows, the MPPS was displaced from 39.2 to 45.3 nm from high flow rates (115 L/min and more) to lower flow rates (85 to 42 L/min). Such tendency is mainly due to the fact that under lower flow rates the diffusion and electrostatic attraction mechanisms are enhanced, while the interception is independent of velocity (Hinds, 1999). This phenomenon causes the intersection of interception and diffusion mechanisms (or interception and electrostatic attraction) to take place at larger sizes. This is consistent with both filtration theory and experimental results (Eninger et al., 2008, Mostofi et al., 2010, 2011).

4.3 Investigation of Particle Loading Effect on Performance of N95 Filtering Facepiece Respirators Performed with Constant and Cyclic Flow

4.3.1 Penetration in Terms of Loading Time

Figures 4-13 to 4-15 indicate the penetration of 10-205.4 nm poly-dispersed particles, performed for the cyclic flow (270 L/min as PIF, 85 L/min as minute volume) and the two constant flows (85 L/min and 170 L/min) selected in this study, for various loading time stages.

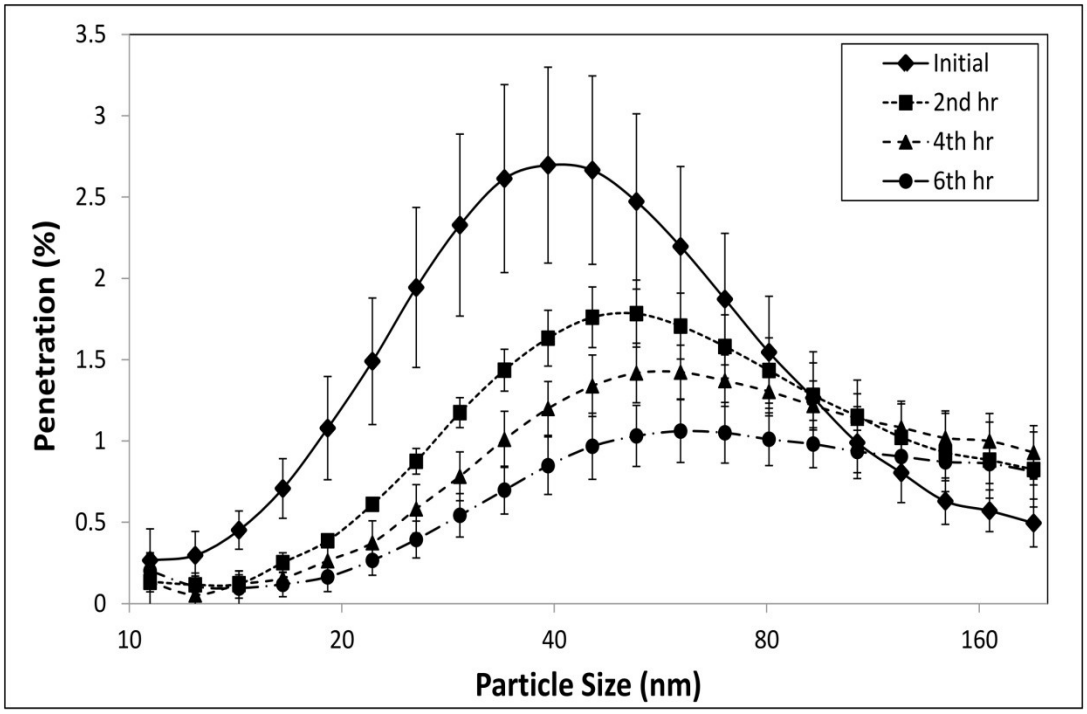

Figure 4-13: Effect of loading time on penetration of NaCl particles through N95 FFRs for constant flow rate of 85 L/min

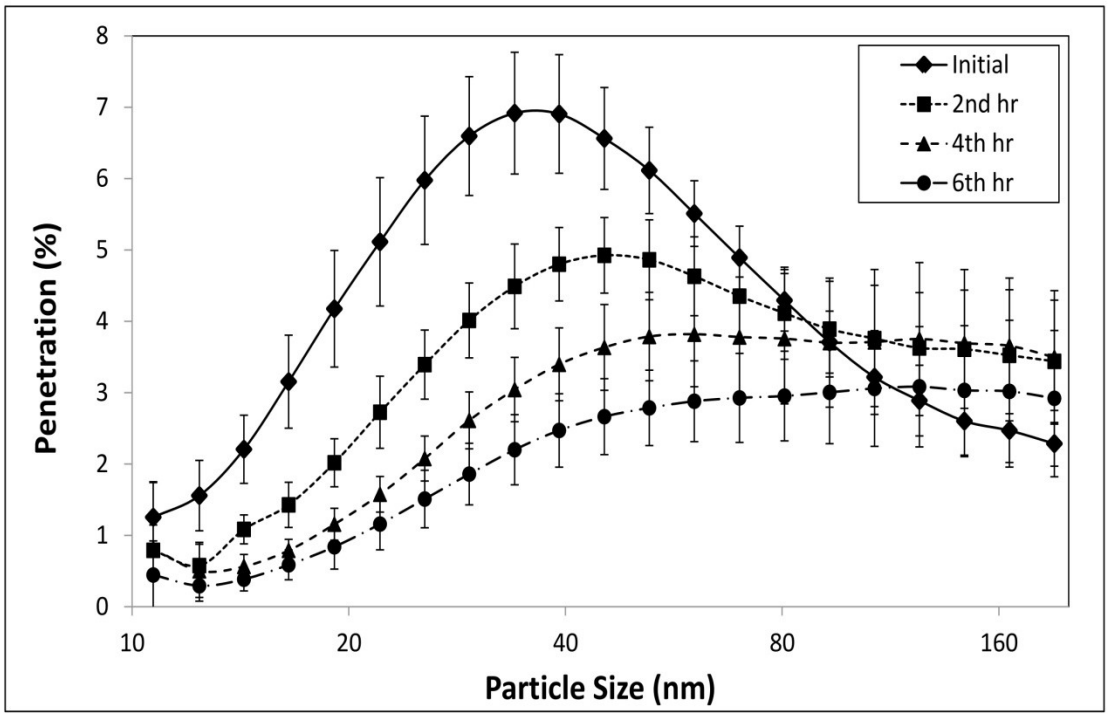

Figure 4-14: Effect of loading time on penetration of NaCl particles through N95 FFRs for constant flow rate of 170 L/min

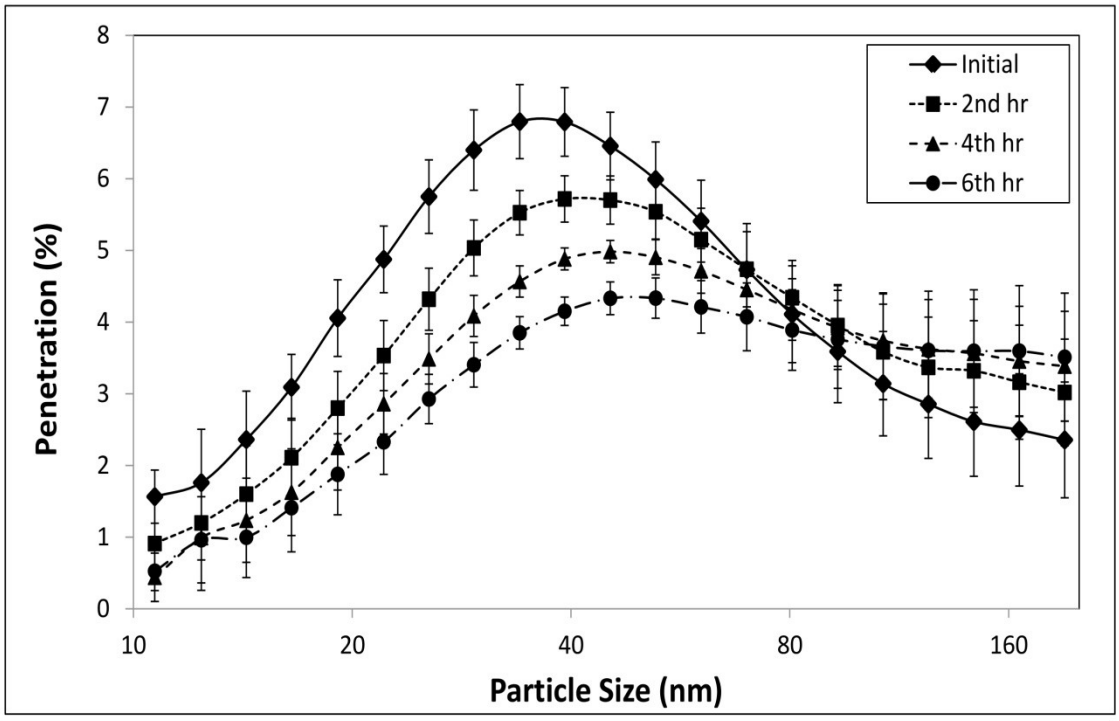

Figure 4-15: Effect of loading time on penetration of NaCl particles through N95 FFRs for cyclic flow (270 L/min as PIF, 85 L/min as minute volume)

As seen in figures 4-13 to 4-15, the penetration for most of the sizes below 100 nm (including MPPS) has been reduced with the loading time under all flow rates. For instance, the maximum penetrations under 85 L/min constant flow rate were reported as 2.7 ± 0.60, 1.78 ± 0.21, 1.42 ± 0.17 and 1.06 ± 0.19 % for the loading times of initial, 2nd hour, 4th hour and 6th hour, respectively. The MPPS was also displaced from 39.2 nm to 60.4 nm from the initial to the final state of loading time (6th hour). The change in maximum penetration in terms of loading time was found to be statistically significant ($p < 0.05$). Similar to the constant flow rate of 85 L/min the penetration of most channels has been significantly reduced ($p<0.05$) for the constant flow rate of 170 L/min. For the 170 L/min, for instance, the maximum penetration was reduced from 6.92 ± 0.85 to 3.08 ± 0.84 % for the initial and final stages of the loading time (6th hour). The MPPS was shifted from 34 to 124.1 nm. Unlike the 85 L/min the shift of MPPS towards larger sizes was found to be more substantial. Also, it was observed that, for the final stage of loading test (6th hour), the location of MPPS could not be sharply visible, since penetration of various size channels (mostly larger than 80 nm) were almost equal and no significant change took place among the penetrations recorded for larger sizes ($p>0.05$). In fact, the penetration curve for the larger sizes at this stage of loading had behaved like a relatively constant function in terms of particle size (see figure 4-14). For the cyclic flow, as occurred for the constant flow rates, the penetration of smaller sizes (mostly <100 nm) was found to be significantly decreased by increase in loading time ($p<0.05$). The maximum penetration for initial and 6th hour stage of loading time for this flow rate was reported as 6.80 ± 0.52 and 4.33 ± 0.28 % respectively. The shift of the MPPS was from

34 to 52.3 nm for the initial and final stage of loading, was found to be less significant compared to constant flow rates.

The reduction of the penetration in nano-metric range and the shift of MPPS towards larger sizes could be attributed to the enhancement of diffusion mechanism, as the filter is loaded with more particles. With such a phenomenon, there is less space for the new particles to diffuse through the filter media and the probability of the collision between particles and the filter fibers (occurred by random Brownian motion) is enhanced. On the other hand, the rate of electrostatic attraction is expected to be reduced, by the loading time (Wang, 2001). However the reduction in the overall penetration (for <100 nm) suggests that, in N95, the increasing impact of diffusion mechanism could overcome the decreasing impact of electrostatic attraction; since the overall penetration has been reduced. All the above findings are interpreted based on experimental data and only for one model of N95 FFRs. Future works on theoretical approach are required to verify any change in filtration mechanisms as a result of loading effect. The reduction in penetration (at nano-metric sizes) is consistent with the results of Moyer and Bergman (2000) and Mostofi et al. (2011).

It is expected that the interception mechanism, in terms of loading time, was less changed compared with the diffusion due to shift of MPPS towards larger sizes instead of smaller sizes. The location of MPPS could be highly dependent of the conjunction of interception and diffusion mechanisms, therefore similar changes in both interception and diffusion could result in no significant displacement of MPPS (which did not occur in this study). The shift of MPPS towards larger sizes, in this study, is not in agreement with the results of Leung et al. (2012). The difference is mainly due to the fact that the behavior of

filtration mechanisms in electrically-charged fibers (as used for N95 and other NIOSH-approved FFRs), could be different from the microfibers or combination of nanofibers and microfibers. The results indicated in this study is, however, based on one model of N95 FFRs. Future works are required to investigate the similarity (or difference) for other types of nano-fiber filter materials.

For larger sizes (usually more than 100 nm) almost a reverse tendency in penetration variations was found compared to nano-sizes. For the constant flow rates of 85 L/min and 170 L/min, the penetration at loading time stages of 2nd and 4th hour was found to be slightly higher compared with their previous stages. For the 6th hour, however, a slight decrease in penetration was observed, compared to the 4th hour. This reduction could be attributed to the formation of dendrites which inhibits more particle penetration. The latter phenomenon is in agreement with literature (Wang, 2001). For the cyclic flow rate, on the other hand, the penetration of the large particles (>100nm) was increased for all the loading time stages compared to their previous stages. The increase in penetration for larger sizes suggests that the electrostatic attraction has been reduced by the loading time (Brown et al. 1988).

4.3.2. Comparison of Constant and Cyclic Flow Penetrations at Initial and Final Stages of Loading Time

Comparison of the penetrations measured by cyclic flows and equivalent constant flows, for N95 filters, has been previously performed by some studies (Gardner et al., 2013, Wang et al., 2012, Eshbaugh et al., 2009, Haruta et al., 2008); however, the measurements were mostly performed for a certain stage of loading time (normally initial penetration). As discussed, one aim of this part was to develop such a comparison when

the loading effect is considered. Figures 4-16 and 4-17 compare the penetration achieved for the selected cyclic flow and the penetrations obtained by the constant flow rates equivalent to minute volume and MIF of the cyclic flow for the two stages of initial and final loading time (0 and 6 hour), respectively.

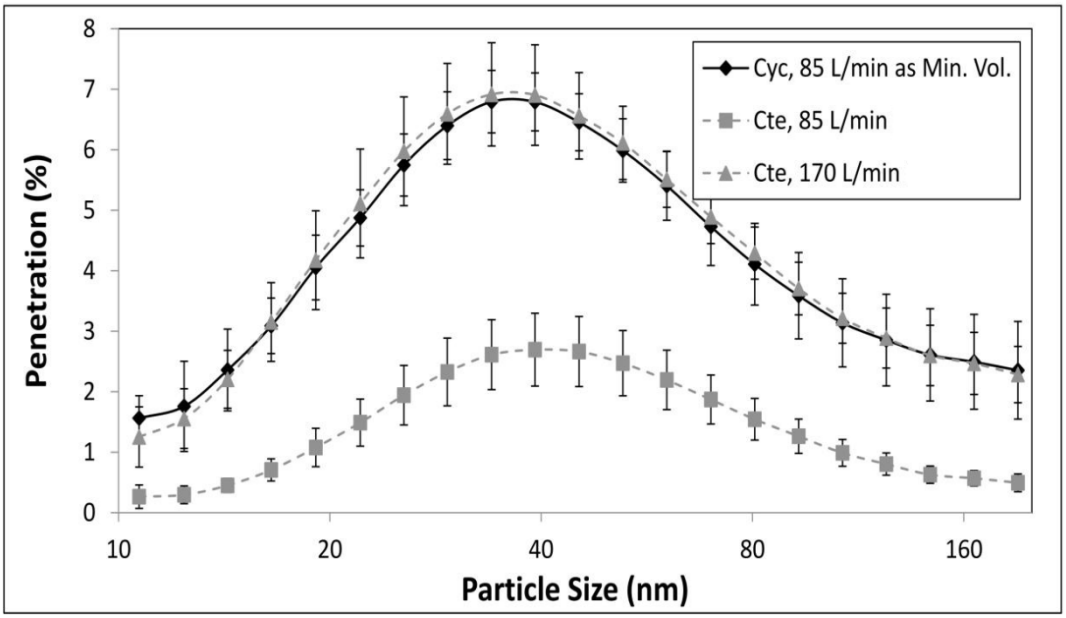

Figure 4-16: Initial penetration of NaCl particles: cyclic flow (270 L/min as PIF, 85 L/min as minute volume); constant flows equal to cyclic flow minute volume (85 L/min) and MIF (170 L/min)

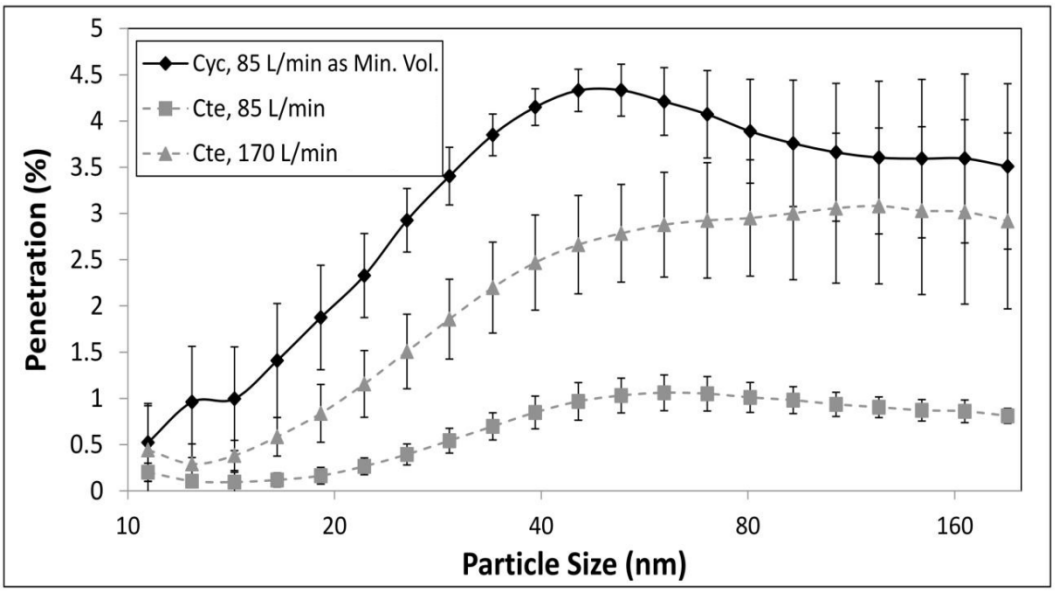

Figure 4-17: Final penetration of NaCl particles: cyclic flow (270 L/min as PIF, 85 L/min as minute volume); constant flows equal to cyclic flow minute volume (85 L/min) and MIF (170 L/min)

As seen in both figures (4-16, 4-17), the penetration under constant flow rate of 85 L/min equivalent to minute volume of the cyclic flow, in both loading time stages is significantly less than the penetration under cyclic flow ($p<0.05$). This indicates that, regardless of the period for which the respirator is exposed by the challenge particles, the constant flow equivalent to cyclic flow minute volume may not accurately represent the penetrations that can be achieved by cyclic flow (which is the realistic case of breathing in human). The latter is consistent with the literature (Wang et al., 2012, Eshbaugh et al., 2009, Brosseau et al., 1990, Stafford et al., 1974).

Unlike minute volume, a constant flow equal to the MIF of the cyclic flow can properly represent the penetration obtained by cyclic flow since penetration curves were almost identical ($p>0.05$) for initial loading time (see figure 4-17). This is consistent with the results of Haruta et al. (2008) for comparison of constant and cyclic flow (with the MIF) rates of 85 L/min. On the other hand, as observed in figure 4-17, the final stage

penetrations under cyclic flow for a wide range of particles (normally within 20- 80 nm) was found to be significantly in excess with the final stage penetrations measured for constant flow (equal to cyclic MIF) ($p<0.05$). Such a difference in constant and cyclic flow penetration could be suggests that the particle loading take place with a slower rate under cyclic flow compared to constant since in cyclic flows. This could be due to the fact that, in cyclic flows, the exposure time is limited to inhalation cycles only (which are half of the respiration cycles). However for constant flow the exposure time is the whole period that the filter is exposed to the particles; therefore particle loading rate is anticipated to be more, as suggested in this study. The increase in cyclic flow penetration compared with constant flow equal to MIF is consistent with the results of Wang et al. (2012) and Eshbaugh et al. (2009). The summary of the results from the two-way ANOVA indicated that, both loading time and flow pattern (cyclic or constant) are significant parameters in variations of the maximum penetration ($p<0.05$). The analysis indicated almost a significant interaction between the two factor variables ($p=0.051$). The interaction between loading time and flow pattern shows that, in different loading time stages, equal or different maximum penetrations could be achieved by constant and cyclic flows.

CHAPTER 5: CONCLUSIONS AND FUTURE WORKS

5.1 Conclusions

Following to the three objectives assessed in this thesis, the findings and conclusions are:

- Objective 1: The contribution of breathing frequency and PIF were investigated in this study with two different experimental setups using one model of N95 FFR. It was concluded that:
    1. PIF had a substantial effect on the UFP penetration while the impact of breathing frequency was limited. The maximum penetration in the MPPS range for the "inhalation and exhalation" experimental setup reached 3.31, 3.66, 7.92 and 9.22% for case A (PIF=135 L/min, Fr=24 BPM), case B (PIF=135 L/min, Fr= 42 BPM), case C (PIF=360 L/min, Fr=24 BPM) and case D (PIF=360 L/min, Fr=42 BPM), respectively. Similarly, 2.99, 3.28, 7.31 and 8.02% penetrations were obtained for the corresponding flows for the "inhalation only" experimental setup.
    2. Statistical analysis indicated that the experimental setup also did not have a significant impact on the penetration ($p>0.05$). However, the results obtained for the setup that included both inhalation and exhalation (setup 1) indicated a slight increase in the penetration that was not observed in the setup with inhalation flow only.
    3. In summary, the experimental results show that among three influencing parameters (PIF, breathing frequency and exhalation flow (setup)), the most significant parameter is the PIF.

- Objective 2: The comparison of penetrations measured for constant and cyclic flows were assessed for a wide range of air flow rate. The following items were concluded:
    1. Among three constant flows equal to the cyclic flow PIF, MIF and minute volume, a constant flow equal to MIF would better represent the penetration for the cyclic flow than the PIF or minute volume.
    2. The comparison between the constant PIF and cyclic flow indicates the constant flow always leads to higher penetrations compared to the cyclic flow. On the other hand, the minute volume is shown to be not high enough to give closed values to the penetration measured under the cyclic flow.
    3. The analysis with the data recorded for the cyclic flow and constant MIF indicates that for the lower flow rates (42-170 L/min) there is no significant difference with the maximum penetration at MPPS between the constant and cyclic flow ($p>0.05$). For 230, 270 and 360 L/min, a significant increase in the maximum penetration was observed by the constant flow rather than cyclic ($p<0.05$).
    4. The two-way ANOVA indicated that both flow pattern (constant or cyclic) and flow magnitude and their interaction can have significant impact on the maximum penetration. ($p<0.05$). This indicated that, according to magnitude of the selected flows, the maximum penetrations obtained between constant and cyclic flow (with equivalent MIF) could be equal or different.

- Objective 3: Loading time was found as a significant item on particle penetration through N95 FFRs. The following items were concluded by objective 3:
    1. The penetration of smaller sizes (usually <100 nm) significantly dropped due to the filter long-term exposure to the challenge particles. The maximum penetration at the initial and final stage of loading time was decreased from 2.7 ± 0.6 to 1.06 ± 0.19 %, 6.92 ± 0.85 to 3.08 ± 0.84 % and 6.80 ± 0.52 to 4.33 ± 0.28 % for the constant flow rates of 85 and 170 L/min and the cyclic flow (with 85 L/min as minute volume), respectively.
    2. A distinct shift in the MPPS was also observed, due to increase of the diffusion mechanism in terms of loading time. At the initial and final stage of loading time, the MPPS was dislocated from 39.2 to 60.4 nm, 34 to 124.1nm and 34 to 52.3 nm for the above selected flow rates, respectively.
    3. The comparison between the cyclic and constant flows for the final stage of the loading revealed that, a constant flow could not predict the penetration of the cyclic flow. Under constant flow (equal to cyclic MIF) the penetration of a wide range of particles, at final stage of loading time, significantly underestimated their corresponding values under cyclic flow.

5.2 Future Works

The following items addresses the limitations of current work and future works are needed to over these limitations.

1- All the findings of this study are limited to only one model of N95 FFRs. However several filter materials (like P-Series and R-Series) are used in the production of

facepiece respirators or cartridges. The investigation of filtration efficiencies should be verified for other filter models and materials, too.

2- The findings of this study, is limited to the proposed experimental setups. However, further theoretical and modeling studies are highly required, to validate the experimental data, and to investigate the impact of all influencing parameters.

3- This study does not address the leakage effects, however in real-world breathing conditions there are two pathways for penetration of particles through filter media: 1-filter media, 2-face-seal leak (Grinshpun et al., 2009). The impact of particle leakage should be considered and its interaction with the findings of this study is highly demanded.

4- The cyclic flows selected in this study, has been all, following sinusoidal pattern, although the respiratory flow pattern in real-world breathing in human can follow various shapes and functions. Future investigation for other patterns of cyclic flow (i.e. trapezoidal, exponential etc) is highly recommended to carry out to investigate the similarities or differences of pattern effects on findings of this study.

REFERENCES

Aitken, R.J., Creely, K.S., Tran, C.L. (2004). "Nanoparticles: An Occupational Hygiene Review". HSE Report 274. Health and Safety Executive, UK.

Anderson, N.J., Cassidy, P.E., Janssen, L.L., Dengel, D.R. (2006). "Peak Inspiratory Flows of Adults Exercising at Light, Moderate and Heavy Work Loads". Journal of the International Society for Respiratory Protection; 23: 53–63.

Balazy, A., Toivola, M., Reponen, T., Podgorski, A., Zimmer, A., Grinshpun, S.A. (2006a). "Manikin-Based Performance Evaluation of N95 Filtering-Facepiece Respirators Challenged with Nanoparticles". Annals of Occupational Hygiene; 50: 259–269.

Balazy, A., Toivola, M., Adhikari, A., Sivasubramani, S.K., Reponen, T., Grinshpun, S.A. (2006b). "Do N95 Respirators Provide 95% Protection Level against Airborne Viruses, and How Adequate Are Surgical Masks?". American Journal of Infection Control; 34: 51–57.

Barrett, L.W., Rousseau, A.D. (1998). "Aerosol Loading Performance of Electret Filter Media". American Industrial Hygiene Association Journal; 59: 532–539.

Berndtsson, G. (2004). "Peak Inhalation Air Flow and Minute Volumes Measured in a Bicycle Ergometer Test". Journal of the International Society for Respiratory Protection; 21: 21–30.

Blackie, S.P., Fairbarn, M.S., McElvaney, N.G., Wilcox, P.G., Morrison, N.J., Pardy, R.L. (1991). "Normal Values and Ranges for Ventilation and Breathing Pattern at Maximal Exercise". Chest; 100: 136–142.

Boskovica, L., Agranovskia, I.E., Altmana, I.S., Braddocka, R.D. (2008). "Filter Efficiency as a Function of Nanoparticle Velocity and Shape". Journal of Aerosol Science; 39: 635– 644.

Brosseau, L.M., Ellenbeker, M.J., Evans, J.S. (1990). “Collection of Silica and Asbestos Aerosols by Respirators at Steady and Cyclic flow”. American Industrial Hygiene Association Journal; 51: 420–426.

Brown, R.C., Wake, D., Gray, R., Blackford, D.B., Bostock, G.J. (1988). “Effect of Industrial Aerosols on the Performance of Electrically Charged Filter Material”. Annals of Occupational Hygiene; 32: 271–294.

Byrne, J.D., Baugh, J.A. (2008). “The Significance of Nanoparticles in Particle-Induced Pulmonary Fibrosis”. McGill Journal of Medicine; 11: 43–50.

Caretti, D.M., Gardner, P.D., Coyne, K.M. (2004). “Workplace Breathing Rates: Defining Anticipated Values and Ranges for Respirator Certification Testing”. U.S. Army ECBC; TR-316. Aberdeen, MD: U.S. Army Research, Development, and Engineering Command.

Chen, C.C., Lehtimaki, M., Willeke, K. (1992). “Aerosol Penetration through Filtering Facepieces and Respirator Cartridges”. American Industrial Hygiene Association Journal; 53: 566–574.

Chen, C.C., Huang, S.H. (1998). “The Effect of Particle Charge on the Performance of a Filtering Facepiece”. American Industrial Hygiene Association Journal; 59: 227–233.

Cho. K.J., Reponen, T., McKay. R., Shukla, R., Haruta, H., Sekar, P., Grinshpun, S.A. (2010). “Large Particle Penetration through N95 Respirator Filters and Facepiece Leaks with Cyclic Flow”. Annals of Occupational Hygiene; 54: 68–77.

Churg, A. (2000). “Particle Uptake by Epithelial Cells. In Gehr, P., Heyder, J., Editors. Particle-Lung Interactions”. New York: Marcel Dekker. pp. 401–435. ISBN 0-8247-9891-0.

DG SANCO. (2004). Nanotechnologies: A Preliminary Risk Analysis on the Basis of a Workshop Organised in Brussels on 1-2 March 2004 by the Health and Consumer Protection Directorate General of the European Commission.

Donaldson, K., Stone, V., Clouter, A., Renwick, L., MacNee, W. (2001). “Ultrafine Particles”. Occupational and Environmental Medicine; 58: 211−216.

Eninger, R.M., Honda, T., Adhikari, A., Heinonen-Tanski, H., Reponen, T., Grinshpun, S.A. (2008). “Filter Performance of N99 and N95 Facepiece Respirators against Viruses and Ultrafine Particles”. Annals of Occupational Hygiene; 52: 385–396.

Eshbaugh, J.P., Gardner, P.D., Richardson, A.W., Hofacre, K.C. (2009). “N95 and P100 Respirator Filter Efficiency under High Constant and Cyclic Flow”. Journal of Occupational and Environmental Hygiene; 6: 52–61.

Fardi, B., Liu, B.Y.H. (1991). “Performance of Disposable Respirators”. Particle and Particle Systems Characterization; 8: 308–314.

Faux, S.P., Tran, C.L., Miller, B.G., Jones, A.D., Monteiller, C., Donaldson, K. (2003). “In Vitro Determinants of Particulate Toxicity: the Dose Metric for Poorly Soluble Dusts”. HSE Research Report 154.

Fjeld, R., Owens, T. (1988). “The Effect of Particle Charge on Penetration in an Electret Filter”. IEEE Transactions on Industry Application; 24: 725–731.

Gardner, P.D., Eshbaugh, J.P., Harpest, S.D., Richardson, A.W., Hofacre, K.C. (2013). “Viable Viral Efficiency of N95 and P100 Respirator Filters at Constant and Cyclic Flow”. Journal of Occupational and Environmental Hygiene; doi:10.1080/15459624.2013.818228.

Grinshpun, S.A., Haruta, H., Eninger, R.M., Reponen, T., Mckay, R.T., Lee, S.A. (2009). “Performance of an N95 Filtering Facepiece Particulate Respirator and a Surgical Mask during Human Breathing: Two Pathways for Particle Penetration”. Journal of Occupational and Environmental Hygiene; 6: 593–603.

Haghighat, F., Bahloul, A., Lara, J., Mostofi, R., Mahdavi, A. (2012). “Development of a Procedure to Measure the Effectiveness of N95 Respirator Filters against Nanoparticles”. Studies and Research Projects / Report R-754, Montréal, IRSST.

Hanley, J.T., Foarde, K.K. (2003). “Validation of Respirator Filter Efficacy”. Report by RTI International, Research Triangle Park, N.C., RTI Contract No. DAAD 19-02-C-0097, Project No. 08621.

Haruta, H., Honda, T., Eninger, R.M., Reponen, T., McKay, R., Grinshpun S.A. (2008). “Experimental and Theoretical Investigation of the Performance of N95 Respirator Filters against Ultrafine Aerosol Particles Tested at Constant and Cyclic Flows”. Journal of the International Society for Respiratory Protection; 25: 75–88.

He, X., Yermakov, M., Reponen, T., McKay, R.T., James, K., Grinshpun, S.A. (2013a). “Manikin-Based Performance Evaluation of Elastomeric Respirators against Combustion Particles”. Journal of Occupational and Environmental Hygiene; 10: 203–312.

He, X., Grinshpun, S.A., Reponen, T., Yermakov, M., McKay, R.T., Haruta, H., Kimura, K. (2013b). “Laboratory Evaluation of the Particle Size Effect on the Performance of an Elastomeric Half-Mask Respirator against Ultrafine Combustion Particles”. Annals of Occupational Hygiene; doi:10.1093/annhyg/met014.

Hinds, W.C. (1999). “Aerosol Technology: Properties, Behavior, and Measurement of Airborne Particles”. (2nd ed.); NewYork: Wiley.

Huang, S.H., Chen, C.W., Chang, C.P., Lai, C.Y., Chen, C.C. (2007a). “Penetration of 4.5 nm to 10 μm Aerosol Particles through Fibrous Filters”. Journal of Aerosol Science; 38: 719 –727.

Huang, H.L., Wang, D.M., Kao, S.T., Yang, S., Hunag, Y.C. (2007b). “Removal of Monodisperse Liquid Aerosols by Using the Polysulfone Membrane Filters”. Journal of Separation and Purification Technology; 54: 96–103.

Hull, M.J., Abraham, J.L. (2002). “Aluminum Welding Fume-Induced Pneumoconiosis”. Human Pathology; 33: 819–825.

ISO/TS. (2009). “Nanotechnologies—Terminology and Definitions for Nano-Objects—Nanoparticle, Nanofibre and Nanoplate”. Geneva, Switzerland: International Standards Organization.

Janssen, L. (2003). “Principles of Physiology and Respirator Performance”. Occupational Health and Safety; 72: 73–81.

Janssen, L.L., Bidwell, J.O., Mullins, H.E., Nelson, T.J. (2003). “Efficiency of Degraded Electret Filters: Part I – Laboratory Testing Against NaCl and DOP Before and After Exposure to Workplace Aerosols”. Journal of the International Society for Respiratory Protection; 20: 71–80.

Janssen, L.L., Anderson, N.J., Cassidy, P.E., Weber, R.A., Nelson, T.J. (2005). “Interpretation of Inhalation Airflow Measurements for Respirator Design and Testing”. Journal of the International Society for Respiratory Protection; 22: 122–141.

Jordan, H.S., Silverman, L. (1961). “Effect of Pulsating Air Flow on Fiber Filter Efficiency”. NYO Report 4814, Harvard School of Public Health, Boston, MA.

Kim, C.S., Bao, L., Okuyama, K., Shimada, M., Niinuma, H. (2006). “Filtration Efficiency of a Fibrous Filter for Nanoparticles”. Journal of Nanoparticle Research; 8: 215–221.

Kim, S.E., Harrington, M.S., Pui, D.Y.H. (2007). “Experimental Study of Nanoparticles Penetration through Commercial Filter Media”. Journal of Nanoparticle Research; 9: 117–125.

Lee, B.U., Yermakov, M., Grinshpun, S.A. (2004). “Unipolar Ion Emission Enhances Respiratory Protection against Fine and Ultrafine Particles”. Journal of Aerosol Science; 35: 1359–1368.

Lee, B.U., Yermakov, M., Grinshpun, S.A. (2005). “Filtering Efficiency of N95- and R95- Type Facepiece Respirators, Dust-Mist Facepiece Respirators, and Surgical Masks Operating in Unipolarly Ionized Indoor Air Environments”. Aerosol and Air Quality Research; 5: 25–38.

Leung, W.W.F., Hunga, C.H. (2008). “Investigation on Pressure Drop Evolution of Fibrous Filter Operating in Aerodynamic Slip Regime under Continuous Loading of Sub-Micron Aerosols”. Separation and Purification Technology; 63: 691–700.

Leung, W.W.F., Hung, C.H. (2012). “Skin Effect in Nanofiber Filtration of Submicron Aerosols”. Separation and Purification Technology; 92: 174–180.

Luo, C.H., Yang, S., Huang, Y.C. (2009). “Removal Efficiency of Bioaerosols by Combining Negative Air Ions with Electrets Filters”. Proceedings of The 11th International Conference on Environmental Science and Technology, Chania, Crete, Greece, September 2009.

Lux Research. (2009). Nanomaterials State of the Market. Q1 2009. Lux Research, Inc., New York, NY.

Mahdavi, A., Bahloul, A., Haghighat, F., Ostiguy, C. (2013). “Contribution of Breathing Frequency and Inhalation Flow Rate on Performance of N95 Filtering Facepiece Respirators”. Annals of Occupational Hygiene; doi:10.1093/annhyg/met051.

Martin, S.B., Moyer, E.S. (2000). “Electrostatic Respirator Filter Media: Filter Efficiency and Most Penetrating Particle Size Effects”. Applied Occupational and Environmental Hygiene; 15: 609–617.

Maynard, A.D., Kuempel, E.D. (2005). “Airborne Nanostructured Particles and Occupational Health”. Journal of Nanoparticle Research; 7: 587–614.

Maynard, A.D. (2007). “Nanotechnology: the Next Big Thing, or Much Ado about Nothing?”. Annals of Occupational Hygiene; 51: 1–12.

Maynard, A.D., Aitken, R.J. (2007). “Assessing Exposure to Airborne Nanomaterials: Current Abilities and Future Requirements”. Nanotoxicology; 1:26–41.

Maynard, A.D., Warheit, D.B., Philbert, M.A. (2011). “The New Toxicology of Sophisticated Materials: Nanotoxicology and Beyond”. Toxicological Sciences; 120(S1): S109–S129.

McCullough, N.V., Brosseau, L.M., Vesley, D. (1997). “Collection of Three Bacterial Aerosols by Respirator and Surgical Mask Filters under Varying Conditions of Flow and Relative Humidity”. Annals of Occupational Hygiene; 41: 677–690.

Morawska, L. (2006). “Droplet Fate in Indoor Environments, or Can We Prevent the Spread of Infection?”. Indoor Air; 16: 335–347.

Mostofi, R., Wang, B., Haghighat, F., Bahloul, A., Lara, J. (2010). “Performance of Mechanical Filters and Respirators for Capturing Nanoparticles – Limitations and Future Direction”. International Journal of Industrial Hygiene; 48: 296–304.

Mostofi, R., Bahloul, A., Lara, J., Wang, B., Cloutier, Y., Haghighat, F. (2011). “Investigating of Potential Affecting Factors on Performance of N95 Respirator”. Journal of the International Society for Respiratory Protection; 28: 26–39.

Moyer, E.S., Bergman, M.S. (2000). “Electrostatic N-95 Respirator Filter Media Efficiency Degradation Resulting from Intermittent Sodium Chloride Aerosol Exposure”. Applied Occupational and Environmental Hygiene; 15: 600–608.

Nel, A., Xia, T., Madler, L., Li, N. (2006). “Toxic Potential of Materials at the Nanolevel”. Science; 311: 622–627.

NIOSH. (1995). Respiratory Protection Devices. Title 42, Code of Federal Regulation, Part 84; Washington, DC: U.S. Government Printing Office, Office of the Federal Register; pp. 30335–98.

Oberdorster, G. (2000). “Toxicology of Ultrafine Particles: In Vivo Studies”. Philosophical Transactions of the Royal Society; London A; 358: 2719−2740.

Oberdorster, G,. Sharp, Z., Atudorei, V., Elder, A., Gelein, R., Lunts, A., Kreyling, W., Cox, C. (2002). “Extrapulmonary Translocation of Ultrafine Carbon Particles Following Whole-Body Inhalation Exposure of Rats”. Journal of Toxicological and Environmental Health, Part A; 65: 1531–1543.

Oberdorster, G., Sharp, Z., Atudorei, V., Elder, A., Gelein, R., Lunts, A., Kreyling, W., Cox, C. (2004). “Translocation of Inhaled Ultrafine Particles to the Brain”. Inhalation Toxicology; 16: 437–445.

Oberdorster, G. (2005). “Nanotoxicology: An Emerging Discipline Evolving from Studies of Ultrafine Particles”. Environmental Health Perspectives; 113: 823–839.

Oh, Y.W., Jeon, K.J., Jung, A.I., Jung, Y.W. (2002). “A Simulation Study on the Collection of Submicron Particles in a Unipolar Charged Fiber”. Aerosol Science and Technology; 36: 573–582.

Ostiguy, C., Soucy, B., Lapointe, G., Woods, C., Ménard, L. (2008). “Health Effects of Nanoparticles”-Second Edition. Studies and Research Projects / Report R-589, Montréal, IRSST, 2008.

Ostiguy, C., Roberge, B., Woods, C., Soucy, B. (2010). “Engineered Nanoparticles: Current Knowledge about Occupational Health and Safety Risks and Prevention Measures” - Second Edition. Studies and Research Projects / Report R-656, Montréal, IRSST, 2010.

Penttinen, P., Timonen, K.L., Tiittanen, P., Mirme, A., Ruuskanen, J., Pekkanen, J. (2001). “Ultrafine Particles in Urban Air and Respiratory Health among Adult Asthmatics”. European Respiratory Journal; 17: 428–435.

Qian, Y., Willeke, K., Grinshpun, S.A., Donnelly, J., Coffey, C.C. (1998). “Performance of N95 Respirators: Filtration Efficiency for Airborne Microbial and Inert Particles”. American Industrial Hygiene Association Journal; 59: 128–132.

Rengasamy, S., King, W.P., Eimer, B.C., Shaffer, R.E. (2008). “Filtration Performance of NIOSH-Approved N95 and P100 Filtering Facepiece Respirators against 4 to 30 Nanometer-Size Nanoparticles”. Journal of Occupational and Environmental Hygiene; 5: 556–564.

Rengasamy, S., Eimer, B.C. (2011a). “Total Inward Leakage of Nanoparticles through Filtering Facepiece Respirators”. Annals of Occupational Hygiene; 55: 253–263.

Rengasamy, S., Miller, A., Eimer, B. (2011b). “Evaluation of the Filtration Performance of NIOSH-Approved N95 Filtering Facepiece Respirators by Photometric and Number-Based Test Methods”. Journal of Occupational and Environmental Hygiene; 8: 23–30.

Rengasamy, S., Eimer, B.C. (2012). “Nanoparticle Penetration through Filter Media and Leakage through Face Seal Interface of N95 Filtering Facepiece Respirators”. Annals of Occupational Hygiene; 56: 568–580.

Richardson, A.W., Eshbaugh, J.P., Hofacre, K.C., Gardner, P.D. (2006). “Respirator Filter Efficiency Testing against Particulate and Biological Aerosols under Moderate to High Flow Rates”. U.S. Army ECBC; CR-085. Aberdeen, MD: U.S. Army Research, Development, and Engineering Command.

Seaton, A., Tran, L., Aitken, R., Donaldson, K. (2010). “Nanoparticles, Human Health Hazard and Regulation”. Journal of the Royal Society Interface; 7: S119–S129.

Semmler, M., Seitz, J., Erbe, F., Mayer, P., Heyder, J., Oberdorster, G., Kreyling, W.G. (2004). “Long-Term Clearance Kinetics of Inhaled Ultrafine Insoluble Iridium Particles from the Rat Lung, Including Transient Translocation into Secondary Organs”. Inhalation Toxicology; 16: 453–459.

Stafford, R.G., Ettinger, H.J., Rowland, T.J. (1973). “Respirator Cartridge Filter Efficiency under Cyclic- and Steady Flow Conditions”. American Industrial Hygiene Association Journal; 34: 182–192.

Steffens, J., Coury, J.R. (2007). “Collection Efficiency of Fiber Filters Operating on the Removal of Nano-Sized Aerosol Particles: I—Homogeneous Fibers”. Separation and Purification Technology; 58: 99–105.

Stevens, G.A., Moyer, E.S. (1989). “Worst Case” Aerosol Testing Parameters: I. Sodium Chloride and Dioctyl Phthalate Aerosol Filter Efficiency as a Function of Particle Size and Flow Rate”. American Industrial Hygiene Association Journal; 50: 257–264.

Teague, E.C. (2004). “Responsible Development of Nanotechnology”. National Nanotechnology Initiative Meeting, April 2, 2004. National Nanotechnology Initiative, 29 p.

Tran, C.L., Buchanan, D., Cullen, R.T., Searl, A., Jones, A.D., Donaldson, K. (2000). "Inhalation of Poorly Soluble Particles. II. Influence of Particle Surface Area on Inflammation and Clearance". Inhalation Toxicology; 12: 1113–1126.

Vincent, J.H., Clement, C.F. (2000). "Ultrafine Particles in Workplace Atmospheres". Philosophical Transactions of the Royal Society; London A; 358: 2673–2682.

Wang, C.S. (2001). "Electrostatic Forces in Fibrous Filters—A Review". Powder Technology; 118: 166–170.

Wang, A., Richardson, A.W., Hofacre, K.C. (2012). "The Effect of Flow Pattern on Collection Efficiency of Respirator Filters". Journal of the International Society for Respiratory Protection; 29: 41–54.

Wichmann, H.E., Spix, C., Tuch, T., Wolk, G., Peters, A., Heinrich, J., Kreyling, W.G., Heyder, J. (2000). "Daily Mortality and Fine and Ultrafine Particles in Erfurt, Germany. Part I: Role of Particle Number and Particle Mass". HEI Research Report No. 98: Health Effects Institute, Boston, MA.

Yang, S., Lee, G.W.M. (2005). "Filtration Characteristics of a Fibrous Filter Pretreated with Anionic Surfactants for Monodisperse Solid Aerosols". Journal of Aerosol Science; 36: 419–437.

Yang, S., Lee, W.M.G., Huang, H.L., Huang, Y.C., Luo, C.H., Wu, C.C., Yu, K.P. (2007). "Aerosol Penetration Properties of an Electret Filter with Submicron Aerosols with Various Operating Factors". Journal of Environmental Science and Health, Part A; 42: 51–57.